THE EFFECT OF MiRNAs ON AUTOPHAGY IN OVARIAN CANCER

Master's Thesis

Stephen Damola ARIYELOYE

Eskişehir 2023

THE EFFECT OF MiRNAs ON AUTOPHAGY IN OVARIAN CANCER

Stephen Damola ARIYELOYE

MASTER'S THESIS

Department of Biochemistry
Supervisor: Prof. Dr. Zerrin SELLER

Eskişehir
Anadolu University
Graduate School of Health Sciences
February 2023

This thesis work was supported within the scope of the project numbered 2110S186, which was accepted by the BAP Commission.

FINAL APPROVAL FOR THESIS

This thesis titled " THE EFFECT OF MiRNAs ON AUTOPHAGY IN OVARIAN CANCER" has been prepared and submitted by Stephen Damola ARIYELOYE in partial fulfillment of the requirements in "Anadolu University Directive on Graduate Education and Examination" for the Degree of Master of Science in Biochemistry Department has been examined and approved on 03/02/2023.

Committee Members	Signature
Member (Supervisor): Prof. Dr. Zerrin Seller	…….
Member: Prof. Dr. Güngör Kanbak	…….
Member: Prof. Dr. Filiz Özdemir	…….

…….

Prof. Dr. Gülşen AKALIN ÇİFTÇİ

Director

Graduate School of Health Sciences

ÖZET

OVARYUM KANSERİNDE MiRNA'LARIN OTOFAJİ ÜZERİNE ETKİSİ

Stephen Damola ARIYELOYE

Biyokimya Anabilim Dalı

Anadolu Üniversitesi, Sağlık Bilimleri Enstitüsü, Şubat 2023

Danışman: Prof. Dr. Zerrin SELLER

Ovaryum kanseri, dünya genelinde kadınlarda en sık teşhis edilen kanser tipleri arasında sekizinci sırada yer almaktadır. Mevcut tedavi yöntemlerinin efektif bir şekilde uygulanmasına rağmen,, ovaryum kanser hastalarının yaklaşık yarısı teşhisten sonra ortalama beş yıl hayatta kalabilmektedir. Bu nedenle, bu ölümcül hastalıkla mücadele etmek için yeni ilaçların, yeni tedavi yöntemlerinin keşfedilmesine ve ovaryum kanserinin mekanizmasının detaylı bir şekilde ortaya konması gerekmektedir. Bu bağlamda,tez çalışması kapsamında ovaryum kanser hücrelerinin (SKOV-3) miRNA-155 ile transfeksiyonu sonrasında hücre ölüm mekanizması olan otofajinin araştırılması amaçlanmıştır.

Bu tez çalışması kapsamında, miRNA-155 mimik ya da miRNA-155 inhibitör transfeksiyonu gerçekleştirilmiş SKOV-3 ovaryum hücre modelleri oluşturulmuştur. Ayrıca, SKOV-3 transfekte edilmiş hücre grupları normoksik ya da hipoksik ortam koşullarında inkübasyona maruz bırakıldıktan sonra farklı konsantrasyonlarda Klorokin ya da Kamptotesin uygulaması yapılmıştır. Oluşturulan bu hücre gruplarında daha sonra hücre göçü oranları, hücre proliferasyonu, otofaji akışı ve morfolojik değişiklikler araştırılmıştır. MiRNA-155'in aşırı ekspresyonu SKOV-3 hücrelerinde proliferasyonu anlamlı bir şekilde arttırken, miRNA-155'in baskılanması ya da Klorokin ya da Kamptotesşn uygulammaları hücre proliferasyonunu belirgin bir şekilde inhibe etmiştir. Aynı şekilde SKOV-3 hücrelerinin hücre göç oranları miRNA-155'in aşırı ekspresyonu sonrasında önemli derecede artış olduğu tespit edilmiştir. Normoksik ve hipoksik koşullar altında, SKOV-3 hücrelerinde miRNA-155 miRNA'nın aşırı ekspresyonunun otofaji oranını azalttığı bunun tersine miRNA-155'in baskılanması ise otofajik yolağın tetiklenmesine neden olmuştur.

Bu nedenle elde edilen sonuçlar, miRNA-155'in SKOV-3 hücrelerinin proliferasyonu dahücre göç oranı da ve otofaji mekanizmasının tetiklenmesinde önemli bir anti-kanser role sahip olduğunu göstermektedir. Bu bağlamda miRNA-155'in baskılanması ile tetiklenen SKOV-3 hücrelerinin otofaji mekanizmasının moleküler düzeyde incelenmesi için detaylı deneysel çalışmaların yapılması öngörülmektedir.

Anahtar Sözcükler: Ovaryum kanseri, Otofaji, miRNA-155, Klorokin, Kamptotesin.

ABSTRACT

THE EFFECT OF MiRNAs ON AUTOPHAGY IN OVARIAN CANCER

Stephen Damola ARIYELOYE

Department of Biochemistry

Anadolu University, Graduate School of Health Sciences, February 2023

Supervisor: Prof. Dr. Zerrin SELLER

Ovarian cancer ranks eighth among the most frequently diagnosed cancer types in women worldwide. Despite the effective application of current treatment methods, about half of ovarian cancer patients survive for an average of five years after diagnosis. Therefore, it is necessary to discover new drugs and new treatment methods to combat this deadly disease and to reveal the mechanism of ovarian cancer in detail. In this context, within the scope of the thesis, it was aimed to investigate autophagy, which is a cell death mechanism, after the transfection of ovarian cancer cells (SKOV-3) with miRNA-155.

Within the scope of this thesis study, SKOV-3 ovarian cell models with miRNA-155 mimic or miRNA-155 inhibitor transfection were created. In addition, transfected SKOV-3 cell groups incubated under normoxic or hypoxic conditions were treated with different concentrations of Chloroquine or Camptothecin. Cell migration rates, cell proliferation, autophagy flux and morphological changes were investigated in these cell groups. Overexpression of miRNA-155 significantly increased proliferation in SKOV-3 cells, whereas suppression of miRNA-155 or administration of Chloroquine or Camptothecin significantly inhibited cell proliferation. Likewise, cell migration rates of SKOV-3 cells were found to increase significantly after miRNA-155 overexpression. Under normoxic and hypoxic conditions, overexpression of miRNA-155 in SKOV-3 cells decreased the rate of autophagy, whereas suppression of miRNA-155 triggered the autophagic pathway.

Therefore, the obtained results show that miRNA-155 has an important anti-cancer role in the proliferation of SKOV-3 cells, the rate of cell migration and the triggering of the autophagy mechanism. In this context, detailed experimental studies are envisaged to examine the autophagy mechanism of SKOV-3 cells triggered by suppression of miRNA-155 at the molecular level.

Keywords: Ovarian cancer, Autophagy, miRNA-155 mimic, Chloroquine, Camptothecin.

ACKNOWLEDGMENT

I would like to thank my esteemed advisor, Prof. Dr. Zerrin SELLER, who supervised my research and shared her vast academic and experimental knowledge and experience with me all through the phases of my research and my master's program. Thanks for your all time encouragement, support, interest, and guidance provided to me as an international student in the department. Thanks for making it easy to study and complete my program in Turkey. I would also like to appreciate your approval for me to participate in the Erasmus+ internship program in Poland and Germany. I am most grateful.

I would like to appreciate Elif APAYDIN for her support and guidance provided during my research project. I want to thank her for her understanding, for patiently helping with my research, for sharing her insights and for waiting to assist me with some of my experimental procedures.

Special thanks to Dr. Öğr. Üyesi Seda Mehtap SARI KILIÇASLAN and Burcu AKY-ILDIZ for the support provided with some of the procedures I used in my research project.

I would like to appreciate Dr. Yüksel ÖĞÜNÇ, Canan Yilmaz, Tayyar Görkem SAYER, Selin DEĞİRMENCİ, Gamze YILMAZ, for making it easy and enjoyable to work together in the same laboratory and for always being helpful and supportive.

I would like to especially appreciate İbrahim Halil ÇELİK and İbrahim YILDIZ my friends who turned brothers. I would like to appreciate their interest and support to me both during my research project and on many other personal notes.

I would like to appreciate my dear parents' Past. Solomon ARIYELOYE and Mrs. To-lulope ARIYELOYE, my brothers Sylvester Adedayo ARIYELOYE, Samuel Adetomiwa ARIYELOYE and Simeon Adeboye ARIYELOYE for their all-time moral, financial and spir-itual support provided throughout my life, my studies in Turkey and my research project.

I would also like to extend my appreciation to my housemate, Rodney KADADI, The RCCG Beautiful Gate parish in Eskisehir, and to every other person who but for space, I could not mention here, who in one way or the other was of immense support to me during the period of my studies.

Last but not least, I would like to sincerely thank the Türkiye Scholarships for providing me with the opportunity to study in Turkey and for funding my Master's degree program. I would like to also thank the Erasmus+ program for funding my studies and all the laboratories that hosted me during the Erasmus program.

My sincere gratitude goes out to you all.

Stephen Damola ARIYELOYE

18/01/2023

STATEMENT OF COMPLIANCE WITH ETHICAL PRINCIPLES AND RULES

I hereby truthfully declare that this thesis is an original work prepared by me; that I have behaved in accordance with the scientific ethical principles and rules throughout the stages of preparation, data collection, analysis, and presentation of my work; that I have cited the sources of all the data and information that could be obtained within the scope of this study, and included these sources in the references section; and that this study has been scanned for plagiarism with “scientific plagiarism detection program” used by Anadolu University, and that “it does not have any plagiarism” whatsoever. I also declare that, if a case contrary to my declaration is detected in my work at any time, I hereby express my consent to all the ethical and legal consequences that are involved.

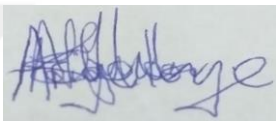

(Signature)

.....

(Stephen Damola ARIYELOYE)

TABLE OF CONTENTS

INDEX OF TABLES

INDEX OF FIGURES

INDEX OF ICONS AND ABBREVIATIONS

α	:Alpha
β	:Beta
κ	:Kappa
μM	: Micromolar
μl	: Microliter
AGO	: Argonaute
Anova	: Analysis of Variance
BRCA1/2	: Genes for susceptibility to breast and ovarian cancer
CI	: Cell index
DGCR8	: Drosha and DiGeorge syndrome critical zone 8
DMEM	: Dulbecco's Modified Eagle's Medium
DMSO	: Dimethyl sulfoxide
DNA	: Deoxyribonucleic acid
EMT	: Epithelial mesenchymal transition
FBS	: Fetal bovine serum
IC50	: Dose constituting 50% of the maximum inhibition
kDa	:Kilo Dalton
MAPK	: Mitogen-activated protein kinase
MiRNA	: microRNA
MTT	: 3-4, 5-dimethyl-thiazolyl-2, 5-diphenyltetrazolium bromide
Myc	: Proto-oncogene
NF-Kb	: Nuclear factor-kappa B
nM	: Nano molar
p53	: p53 protein
pre-miRNA	: Precursor miRNA
pri-miRNA	: Primary miRNA
RAS	: a proto-oncogene of the G-protein type
RISC	: RNA-induced silencing complex
RNA	: Ribonucleic acid
RTCA	: Real Time Cell Analysis
SEM	: Standard mean error
SKOV-3	: Human ovarian cancer cell line
TRBP	: Trans-activation response RNA-binding protein

UTR : Untranslated regions

1. INTRODUCTION

Cancer is a major world problem. It is of a huge concern globally. Statistics shows that it's a leading cause of morbidity globally. As reported by the World Health Organization, more than 17 million people worldwide suffer from this disease and about 10 million deaths from cancer were documented globally in 2018. Sadly, up till now, cancer chemotherapy has not proven most effective. It's been repeatedly shown to give some side effects that aren't too beneficial to the health of patients and also linked to poor patient outcomes (Ashrafizadeh et al., 2021; Khaiwa et al., 2021).

Ovarian cancer takes the eight places in the ranking of the most diagnosed tumors. There has been a record of about 185,000 women in the world who die as a result of this disease yearly. There is a little difference in the survival rate of different ovarian cancer type. Serous ovarian carcinoma has 43% survival rate, endometrioid 82%, clear cell 66%, and mucinous 71% (Provencher et al., 2000; Barnes et al., 2020).

Hypoxia has been reported to be connected with poor prognosis because it encourages resistance to chemotherapy or immunotherapy, increases malignancy potential, and also the occurrence of metastasis. The tumor microenvironment composes of signaling molecules, blood vessels, an extracellular matrix, and non-malignant cells such as immune cells fibroblasts, and stromal cells. In contrast with normal tissues, the vasculature of solid tumors is dysfunctional. Immune cell functions in tumors are hindered by the hypoxic environments of tumors which are formed from vasculature pathology, tumor growth rate, and the composition of the stroma (Boulefour et al., 2021).

In addition, hypoxia encourages cells with the potential for malignancy as a result of altered genetic makeup to grow due to the pressure it exerts on these cells. Hypoxia, therefore, stimulates the motility and metastasis of cells because it facilitates epithelial-to-mesenchymal cell transition (EMT). Hypoxia also induces cell quiescence by disturbing the metabolism of tumor cells. It can lead to the Frapy resistance by altering the distribution and/or transport of immunotherapy, chemotherapy, and radiotherapy. Numerous studies are currently focusing on how tumor cells, therapies, and clinical outcomes are being affected by hypoxia. Some strategies to overcome hypoxia are currently being developed (Boulefour et al., 2021).

MicroRNAs (miRNAs) are a type of small non-coding RNAs with a primary function of regulating the expression of targeted messenger RNA (mRNA) transcripts. Cancer develops once these miRNAs have impaired expression and this includes ovarian cancer (Lopacinska-Jørgensen et al., 2021). MiRNAs have a part to play as an important regulator in very many

physiological phenomenon such as cellular metabolism, signaling pathways regulation, embryonic development and tissue differentiation (Zou et al., 2021). MiRNAs are now being employed as signatures to detect certain types of diseases and to develop various therapies. Estimates are suggesting that miRNAs have the potential to regulate up to 60 % of human genes. The most recent finding on miRNAs reported that 1917 annotated hairpin precursors can be derived from the human genome and 2654 mature sequences can be generated from these precursors (Zou et al., 2021).

The number of true mature miRNAs in humans has been reported to be around 2300 and each of these has the capacity to target thousands of mRNAs and thus, thousands of biological events. MiRNA biogenesis is not a single event (Hyttinen et al., 2021).

A major challenge betiding the clear assertion of the roles of miRNAs in tumorigenesis is the absence of many methods that help with the identification and validation of miRNA-mRNA pairing and consequence. Although many tools are currently being developed and improved upon for the computational prediction of miRNA targets, some of the obtained results may be wrongly interpreted. Due to the cost, time and perhaps energy demands attached, it still looks unlikely to be able to validate experimentally all of the predicted potential miRNA-mRNA pairs (Lopacinska-Jørgensen et al., 2021).

Autophagy is a self-degradative process happening mostly in eukaryotic cells and it occurs to clear up proteins or organelles in cells that are damaged or that aren't functioning properly. It is such a dynamic process that is able to help maintain the homeostasis of cells and also regulate metabolic stress response (Zhou et al., 2020). Autophagy acts differently depending on certain factors. It may result into unintended consequence such as; to some cancer suppressing effects or some cancer promoting effects. One effect might come from the genomic instability and degradation of important cellular component that causes autophagy to inhibit the growth of tumors and lead to abnormal transformations that ultimately results in apoptosis. The other effect might result from the recycling and clearance of damaged or dysfunctional proteins and organelles that serve as an energy resource for tumor cells. This allows cellular homeostasis to be maintained and allows the cancer cells to develop resistance against chemotherapy and radio therapy (Zou et al., 2021).

It is therefore important to target autophagy as a way to overcome resistance to drugs and improve the outcomes of anticancer therapies for patients. Tumor cells exploit the autophagy pathway to compensate for survival. Targeting autophagy has been a long central part of combinational cancer therapeutic strategy (Zhou et al., 2020).

A consortium of studies that would help to provide a more comprehensive insight into the relationship between the different signaling networks that contribute to the sustenance of sensitivity or resistance to drugs is crucially needed at this time (Ashrafizadeh et al., 2021). In the quest to find inhibitors of autophagy, chemical inhibitors such as Chloroquine (CQ) and hydroxyl chloroquine (HCQ) are now under clinical trials. But as it is, each of these candidate drugs lacks enough capacity to significantly inhibit autophagy alone and be employed as a monotherapy. As a result of this, the race still continues in the search for more effective approaches to inhibiting autophagy (Liang et al., 2020).

A notable approach that has been recently reported to have a promise of specifically inhibiting autophagy is the miRNA-based approach. In this thesis, we focused on the modulatory role of miRNA-155 on autophagy in ovarian cancer SKOV-3 cells (Liang et al., 2020; Lin et al., 2022).

2. LITERATURE REVIEW

2.1. Cancer Biology

Today, many definitions could be lent to describe cancer based on its complex modality and form. Oncology, the study of cancer, a major and leading cause of human death, is very important and must continually be studied until it is fully understood and conquered. An early detection, coupled with appropriate intervention can go a long way in facilitating cancer survival. Despite the many progresses recorded in cancer treatment, treatment ineffectiveness, constitutive side effects, the inability to tailor treatment regimens to address individual patient need and drug resistance make up the current cancer therapy critical challenges (Sabzpoushan, 2020).

Cancer is marked by many events, some of which includes; angiogenesis, metastasis, invasion, tumor-supported inflammation, apoptosis, uncontrolled growth, programmed cell death, immune attack and growth suppressors evasion, unrestrained energy use, continued proliferation and genomic mutation or compromise and instability (Sabzpoushan, 2020). Several machineries could be implicated in cancer etiology, such as unfavorable environmental or exogenous conditions, cell cycle errors, viral infection. such as Hepatitis B infection, Hepatitis C infection, Human Papilloma Virus infection, certain kinds of lifestyles (Diori Karidio and Sanlier, 2021). One of the open questions that could be exploited for therapeutic development is how to manage metastasis, since primary tumors or neoplasms are considerably manageable (Diori Karidio and Sanlier, 2021).

The balance and or regulated expression of certain type of genes such as the oncogenes, proto-oncogenes and tumor suppressor genes are very critical for normal homeostasis. An alteration in this has been implicated in various cancer types. Identifying and characterizing these genes, their products, their behaviors under certain conditions as well as their interactions with other elements provides a wealth of information for cancer diagnosis, prognosis and therapeutic development. Examples of such important genes include p53 gene, Her2/neu gene, APC, ras, myc, DCC and Rb (Kontomanolis et al., 2021). Over the years and despite the increasing efforts made to combat cancer, from many quarters, cancer has successfully widened its scope; type, form, mechanism and resistance to therapy. The past decade has recorded a whooping percentage of over 25% novel cancer therapies ratified by the Food and Drug Administration, surmounting the previous records from the 1980s, the beginning of the upsurge of genomic technologies. There has been a chase for the invention of new therapeutic strategies that borders around chemo, immune, targeted molecular therapy, surgery and radiation such as addressing

undruggable targets that results in degradation (proteolysis targeting chimera (PROTAC), using improvised or adaptive strategies for hematological-cum-solid tumors (novel chimeric antigen receptor (CAR)-T, and manipulating part of the RNA transcription facilities to achieve mechanistic epigenetic control for tumor growth and resistance (Guan et al., 2020 ; Ruggeri, 2021).

2.2. Ovarian Cancer

Ovarian cancer is known as a 'deadliest gynecological cancer'. Only about 48.8% of its patients survive it in 5 years- post development. This is due to its asymptomatic tendencies of its early stages of development. One of the major predicaments of ovarian cancer is its late diagnosis. Most (~90%) of the women with epithelial ovarian cancer are diagnosed when the cancer is in its advanced stages. However, if diagnosis is made earlier, such as the stage I ovarian cancer without metastasis, the rate of survival in 5 years could be as high as ninety percent (90%) (Carey et al., 2021). There are two major precursor cells to ovarian cancer; the first is the ovarian surface epithelium and the other is the fallopian tube epithelium. The precise route by which these two precursor cells are mutationally transformed has yet to be unraveled. It remains an enigma (Hallas-Potts et al., 2019; Shukla and Singh, 2021; Hallas-Potts et al., 2019).

At the onset of ovarian cancer development, the loss or change of the normal epithelial cell phenotype constitute the most critical step of the process initiation. Usually, a normal ovarian surface epithelium cell is characterized by its possession of both epithelial and mesenchymal configuration, and a normal fallopian tube epithelium possesses only an epithelial configuration. However, as ovarian cancer developmental process begins, both ovarian surface epithelium and fallopian tube epithelium cells through the process of epithelial-mesenchymal transition (EMT) gain a more stable mesenchymal phenotype. The epithelial microcosm is made up of cells conjoined by lateral cell–cell connections that contain the desmosomes, adherens and tight junctions that help sustain the epithelial integrity and regulate movements. The connection of tight and adherens junctions results in a belt formation between epithelial cells (Hallas-Potts et al., 2019; Shukla & Singh, 2021).

One of the earliest markers of the EMT process is the breakdown of the tight junction assembly causes the transmembrane proteins anchored in the epithelial cells to be re-arranged. Moreover, the adherens junction assembly is also compromised and this results in further events that ultimately rearrange the cytoskeleton and lead to a less stable phenotype acquisition. Mesenchymal phenotypes have been reported to have an increased rate of migration, invasion,

and production of Extracellular matrix constituents. It has been established through reports that the mesenchymal transformation of a cell is enough for the metastasis of cancerous cells. As E-cadherin a major epithelial cell marker is lost, vimentin and N-cadherin mesenchymal proteins are gained. This transition comes with a cuboidal to elongated spindle conformational changes in cell shapes (Hallas-Potts et al., 2019; Shukla & Singh, 2021).

In ovarian cancer metastasis, a strong adhesion of ovarian cancer cells to the mesothelial monolayer that borders the peritoneum is observed. Several proteins have been implicated in this facilitation, such as the mucin 16 surface-associated protein that houses the Ca125 antigen. After the establishment of metastatic environment adherence, aniokis-resistant cells of the ascites changes configuration and becomes prolific. A state that enables them to relate with the microenvironment of the omentum and peritoneum, by exploiting the mesenchymal-epithelial transition process. A good invasion of cells is predicated on the smooth interaction of metastatic cancer cells and the tumor microenvironment. Furthermore, in the later course of ovarian cancer cells metastasis, new blood vessels are created from already existing vasculature, a process termed as angiogenesis. This critical step in metastasis, enables both primary and metastatic tumor growth to grow beyond the diffusion-limited largest size of about $2mm^3$ (Carey et al., 2021) has revealed that several metalloproteases are involved in this progression (Carey et al., 2021).

2.2.1. Ovarian cancer risk factors

Ovarian cancer is implicated by various risk factors and could be ameliorated by other factors. Examples of risk factors for ovarian cancer include ageing, menopause, post menopause hormone therapy (e.g estrogen and progesterone use has a relative risk of 1.53 and confidence interval of 1.40-1.66), hormone imbalance, obesity, weight gain, endocrine disruptors, chemical substances, occupational risk factors, gene mutation, environmental risk agents, hereditary maladies having a germline disruption of BRCA1and BRCA2 genes predisposes not only to ovarian cancer, but to other cancer types, such as breast cancer. Sometimes, some women have no maternal family record of ovarian cancers, yet they still inherit these BRCA gene mutations from their fathers. About 25% of ovarian cancers have been reported to host mutations in either or both of these two genes. Hereditary colon cancer, metabolic syndrome, adenine DNA glycosylase (MUTYH)- associated polyposis syndrome, polycystic ovary syndrome, Peutz-Jeghers syndrome, and many more are other ovarian cancer related hereditary

maladies. Lynch syndrome with mutations in the PMS2, MSH2, MSH6, mismatch repair system genes are also some examples of genetic risk factors of ovarian cancer (Falzone et al., 2021; Ibragimova et al., 2021).

Developed regions of the world such as Europe and North America has been reported to have the highest number of cases. Ovarian cancer in Europe and the United States of America, is ranked fifth, in the cause of women's death. The mortality from this disease depends many factors such as the availability and access to diagnostic and therapeutic options, with the African populations having to suffer the most death cases. Lack of recreational activities, age at menarche, poor diet, and many more have been also noted as a factor in ovarian cancer disease. Of these, a high body mass index (BMI) and smoking were discovered to exacerbate the survival rate. White-skinned people are non-Hispanic record the highest ovarian cancer cases of about 5.2 per 100,000 while those who are black-skinned non-Hispanic and Asians/Pacific Islanders record the lowest number of cases or incidence of about 3.4 per 100,000 (Ibragimova et al., 2021; Gaitskell et al., 2022).

A wide difference has been documented between African American (AA) and Caucasian American (CA) women with ovarian cancer. While Hispanic and Asian women are not largely diagnosed with advanced ovarian cancer but at a younger ages, with more END and CC subtypes than CA/AA women, AA women have a higher death rate due to ovarian cancer. AA women are also diagnosed lately, with more recurrence and less disease-free survival rate (Shukla & Singh, 2021). This disparity could also be as a result of variations in the mitochondrial genetic composition of these races (Shukla & Singh, 2021) . Use of tobacco smoking, talc powder, diet and androgens make up some other unratified ovarian cancer risk factors. Meanwhile, pregnancy and breastfeeding has been identified as a major factor for reduced ovarian cancer incidence. Women with full-term pregnancies before the age of 26 have been observed to have a considerable minimal risk of developing the disease. This is further reduced by the time used to breastfeed. Oral contraceptives, tubal ligation, use of the intrauterine devices for birth control have also been noted to reduce ovarian cancer incidences (Falzone et al., 2021).

2.2.2. Symptoms of ovarian cancer

Early or mild stage ovarian cancer symptoms can be easily confused with other conditions that are benign, such as benign ovarian lesions (Fibromas, ovarian cysts and teratomas), gastrointestinal and urogenital disorders. It must be noted that, when ovarian cancer symptoms develop truly, they are persistent and they usually get worse with time. Examples of these symptoms may include pelvic and abdominal pain, urgent and frequent passing of urine, pelvic

distention. Back pain, pain during sex, weight loss, altered menstruation, fatigue and constipation are also further examples if ovarian cancer symptoms (Falzone et al., 2021).

There are several prognostic and diagnostic employed for detecting ovarian cancer or its possible occurrence, especially in case of abdominal pain and presence of other benign pathologies. A fast resource to quickly consort is the patients' medical and family history. In addition to physical examination, certain laboratory tests are also of great importance in ovarian cancer diagnosis. A good example apart from testing for the typical hematochemical parameters is testing for the cancer antigen (CA) 125 and human epididymis protein 4 (HE4) which are purported markers found in the blood of ovarian cancer patients. CA 125 is well reported as a major serum marker used for diagnosing patients with ovarian cancer. It is highly elevated in early-stage patients (50%) and in patients with fully developed tumor (over 80%). After assertion has been made by these and other preliminary tests, imaging tests are further performed such as ultrasound, magnetic resonance imaging (MRI) scan, computed tomography (CT) scan etc. Furthermore, molecular tests that screen for mutations in BRCA1, BRCA1, MLH1 and other genes are employed to comprehensively diagnose, counsel and/or manage ovarian cancer (Falzone et al., 2021).

2.2.3. Treatment of ovarian cancer

Recently, several therapeutic routes are being employed in the management of ovarian cancer. These therapeutic options depend on the cancer stage, response to and or relapse. Examples include minimally invasive and open surgeries, use of first, second and third-line chemo and or immune targeted therapies like platinum and non-platinum-based treatments. Carboplatin, gemcitabine, bevacizumab, topotecan, doxorubicin, and many others are now popularly used therapeutic agents in ovarian cancer management. These treatment options have over the decades proven, to say the least, to significantly improve the quality of life and the life expectancy of those with the disease. A popular trend has been a combined use of these options (Falzone et al., 2021; Pundir et al., 2022). More recently, in the treatment of advanced ovarian cancers, novel therapeutic options such as adoptive cellular therapy, T cell transfer, therapeutic vaccines, and chimeric antigen receptor T-cell therapy are being developed and their safety level is being evaluated (Falzone et al., 2021; Pundir et al., 2022).

Formerly, ovarian cancer was been managed stereotypically by surgeons, pathologists and medical oncologists, without a collaborative effort for better treatment regimens. However, this individualized treatment option limits ovarian cancer treatment. More recently, a collaborative-cum-integrative approach has been employed in ovarian cancer management. Besides

the aforementioned specialist, a multidisciplinary team has proven to improve treatment outcomes. More specialist such as the nutritionist, urologist, geneticist, vascular surgeon and many more are being employed to together manage the disease and from records, it turned out to pay off. While the patient is kept at the center, a network of treatment specialist is formed, who share information based on their competence and expedite the most effective treatment implementation with personalized medicine (Falzone et al., 2021). Figure 2.1 gives an overview of the reproductive system of women and the ovarium biology.

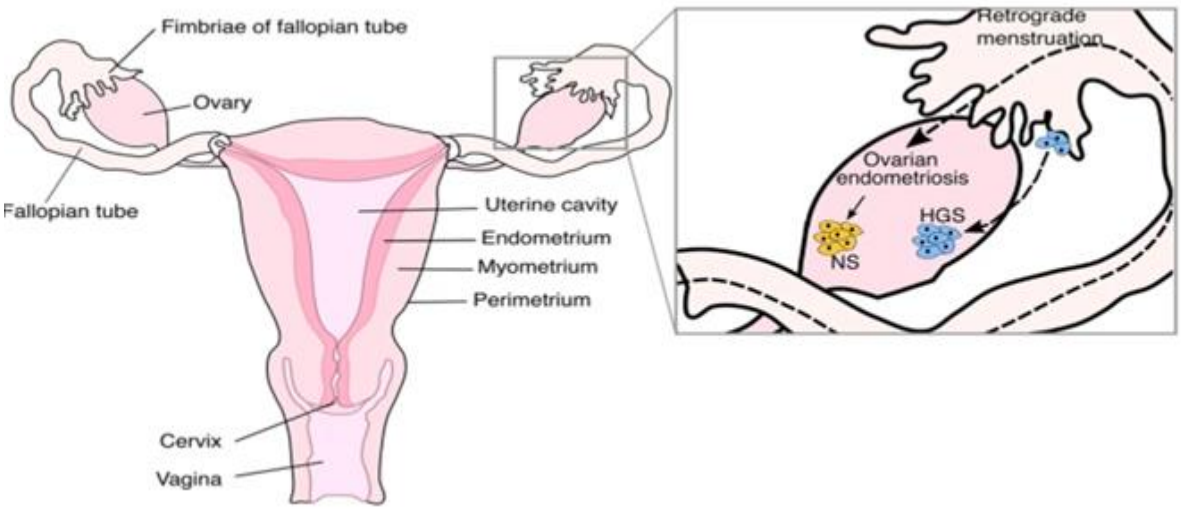

Figure 2.1. *Cancer biology of the ovary and anatomy of the reproductive system (Hallas-Potts et al., 2019)*

2.2.4. SKOV-3 cell line

SKOV3 cells were found by Hallas-Potts et al., 2019 to be one of the most invasive out of the 11 ovarian cancer cell lines analyzed in their study. It was also grouped as a non-serous ovarian cancer type, together with the likes of A2780, OVCAR8, TOV21G and OAW42. SKOV3 has its origin from ascitic fluid and its high invasive character stems from the highly invasive nature of ascites, which are usually formed at advanced disease state (Hallas-Potts et al., 2019). SKOV3 cell line has been in the forefront of use in most ovarian cancer studies. This is in turn followed by the A2780, ovarian cancer cell line, then the OVCAR-3 cell line, the IGROV-1, CAOV-3, 59M cell lines and lastly in order of most usage, OVCAR-8 (Hallas-Potts et al., 2019).

2.3. Autophagy

Autophagy basically is a catabolic pro-survival or cell death mechanism characterized by lysosomal degradation or destruction of foreign entities in the cell and/or cytoplasmic components such as proteins, damaged cellular organelles and other macromolecular structures. Autophagy literally translates to" to eat oneself". This cell death mechanism is made possible when the autophagosome interacts with the lysosome to bring about the degradation of its cargo, most times releasing energy for cell consumption. For this function and its control, autophagy related genes are employed (Wu et al., 2020; Santagostino et al., 2021; Miller et al., 2020; Tilija Pun et al., 2020).

Several factors have been documented to bring autophagy to bear, a few examples of these include; hypoxia, ER stress, nutrient and growth factor deficiency or starvation, drug treatment, reactive oxygen species (Patil et al., 2020). Autophagy with cell death could be reviewed under three contexts:

a. Cell death in which autophagy connects with apoptosis at the same time or in parallel, called autophagy associated cell death.
b. Cell death where autophagy precedes other cell death kinds, referred to as autophagy mediated cell death.
c. Cell death that is totally dependent on autophagy, referred to as autophagic death or autophagy dependent cell death (Chen and Gibson, 2021).

The autophagy at cellular level could be summarized as follows; after autophagy has been stimulated in the cells by various autophagic stimulating factors, a double membraned phagophores which originates from the lipid bilayers of structures such as the plasma membrane, mitochondria, Golgi apparatus is formed. This newly formed phagophore further expands to enwrap contents of the cell such as proteins, ribosomes and other organelles. Once these cargoes are loaded into the phagophore, a double membraned structure called autophagosome is formed. The autophagosome further interacts with the lysosome to produce an autolysosome, and this interaction facilitates the breakdown or degradation of the autophagosomal contents by the lysosomal acid proteases resident in the lysosome. Lastly, after degradation, the degraded byproducts through the agencies of transporters and permeases in the lysosome are recycled back into the cytoplasm. These degraded products can now be used for metabolism or for the construction of new macromolecules (Tilija Pun et al., 2020).

In molecular terms, autophagy can be graphically illustrated in five stages, namely; (a) initiation, (b) elongation, (c) maturation, (d) fusion, and (e) degradation.

(a) Initiation: The Unc-51-like kinase (ULK) complex made up of ULK, Atg13, FIP200 and Atg101, molecularly speaking is responsible for initiating autophagy. Changes in ULK1 via auto or dephosphorylation and in Atg13 triggers the autophagy pathway. On the contrary, ULK1/2 and Atg13 are inactivated once the mammalian target of rapamycin (mTOR) complex1 (mTORC1) is activated. This intrinsically results in autophagy inactivation. An important element in autophagy Beclin1-Vps34-Atg14L-p150 complex, upon ULK1 activation is subsequently activated when ULK1 phosphorylates Beclin 1. The result of this process produces phosphatidylinositol-3-phosphate, a very important autophagic vesicle nucleation element (Tilija Pun et al., 2020).

(b) Elongation: Once autophagy has been triggered by the activation of the foremost mentioned autophagic elements, two ubiquitin-like conjugation systems come into play, namely; Atg12 System and a light chain (LC3) system also referred to as microtubule-associated protein 1 light chain 3. First, with the help of two enzymes E1 (Atg7) and E2 (Atg3) enzymes, Phosphatidylethanolamine (PE) is conjugated by LC3 to form an LC3-Phosphatidylethanolamine (PE) conjugate which is soluble. The soluble LC3-Phosphatidylethanolamine (PE) conjugate then becomes non-soluble and hence referred to as the non-soluble (LC3-II) form. This new form is further inserted firmly into the autophagosome membrane (Tilija Pun et al., 2020).

Second, E2 Enzymes (Atg5byAtg7andAtg10) are conjugated to the Atg12 system and result in the formation of Atg12-Atg5heterodimer. Atg12-Atg5heterodimer in turn forms a complex through its interaction with Atg16L. This new complex has an important role in the elongation of the autophagic membrane. The cellular element or cargo to be engulfed is usually selected partly by a phenomenon called targeted ubiquitination. The LC3-interacting region of p62 subsequently directs the integration of the cargo of choice into the autophagosome. Furthermore, the incorporation into the outer and inner membrane of the autophagosome of phosphatidylethanolamine lipidated LC3 (LC3II) takes place after which the intraluminal LC3II is digested together with the cargoes, while the cytosolic LC3II are de-lipidated (Tilija Pun et al., 2020).

(c) Maturation and (d) fusion: After the formation of the autophagosome and its maturation, the autophagosome via molecules such as Rubicon, SNAREs, UVRAG, LAMP, Rab7, etc. fuses with the lysosome and the early and late endosome. This is termed autophagy flux or autophagosome maturation. SNAP receptors complex (SNAREs), Rab GTPases and tethering

factors are 3 important proteins that have been documented to aid effective autophagosome-lysosome fusion (Tilija Pun et al., 2020).

(e) Degradation: Finally, the cargos delivered to the lysosomes are degraded via lysosomal hydrolases. The end products are further recycled into the cytosol via lysosomal permeases for reuse by the cell. Figure 2.2 gives an overview of the stages involved in autophagy.

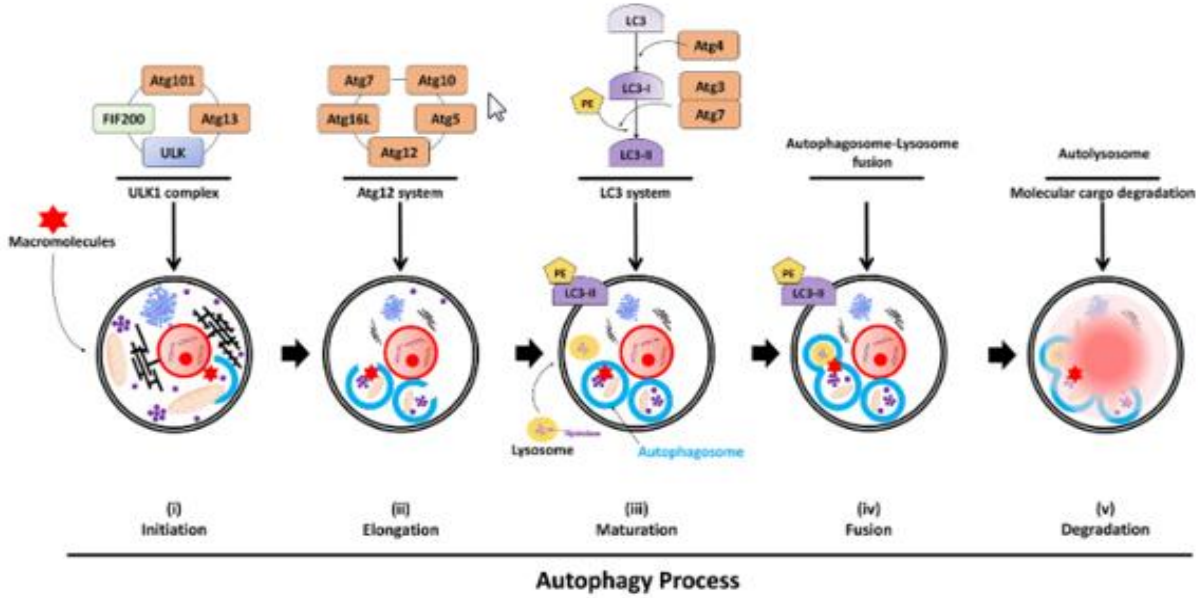

Figure 2.2. *Stages of autophagy (Patil et al., 2020)*

2.3.1. Types of autophagy

Autophagy could be further classified into different types, based on how the cellular cargo is made available to the lysosome for destruction. Examples include the macroautophagy, microautophagy, the chaperone- mediated autophagy (CMA). Macroautophagy is the most prevalent of these subtypes, it spans from delivering the cytoplasmic components into the autophagosome and later degraded by lysosomal enzymes (Chen and Gibson, 2021). Under microautophagy, the cytoplasmic cargo directly invades the lysosome to be delivered. CMA on the other hand employs heat shock cognate protein (hsp70) to selectively give proteins with KFERQ-like pentapeptide to the lysosome (Tilija Pun et al., 2020).

Parallel to the cytotoxicity that hypoxia causes in cells, it also modifies the metabolic profile of cells under its influence. Various cellular components under hypoxic stress as reported in many cases are being degraded by autophagy to produce different autophagy types

based on the components affected, including ribosomes (ribophagy), mitochondria (mitophagy), lipids (lipophagy), peroxisomes (pexophagy), nucleus (nucleophagy), and ER (ERphagy or reticulophagy). Unfortunately, the significance and precise mechanism governing the different forms of selective autophagy under hypoxic stress are still not clear and need to be studied for clarification (Tilija Pun et al., 2020).

2.3.1.1. *Selective autophagy*

Selective autophagy works to control how a number of specific cell elements are degraded. It does this through the action of some particular autophagic receptors such as the nuclear dot protein 52 kDa (NDP52), p62/SQSTM1, valosin-containing protein (VCP) e.t.c. These receptors that are autophagy related have a specific recognition capacity for cargos that have been ubiquitinated and thereby allows for their elimination via the LC3/ GABARAP/Gate16 protein interaction on the phagophore membrane. Selective autophagy has been found to function as a tumor-suppression mechanism at the earlier stages of cancer development. However, it is also being reported to exhibit some tumor survival and protective functions through its prosurvival mechanism (Rakesh et al., 2022).

2.3.1.2. *Macroautophagy*

Macroautophagy involves the formation of phagophores and autophagosomes upon the interaction with the organelles with a LC3-II form. The damaged organelles in the phagophore is carried by the autophagosome to the lysosome where it fuses to form the autophagolysosome. The damaged organelles are subsequently lysed in the lysosome through the activity of acid hydrolases (Rakesh et al., 2022).

2.3.1.3. *Microautophagy*

Microautophagy undertakes the selective and non-selective autophagy paths. While the selective pathway requires chaperones to interact with substrate proteins and move into the lysosome, non-selective autophagy rather requires both the organelles and proteins to enter the lysosome where acid hydrolases detoxify them (Rakesh et al., 2022).

2.3.1.4. *Mitophagy*

Mitophagy utilizes either the Parkin dependent or parkin independent pathways to destroy defective mitochondria. PINK1 interacts with PARL during the Parkin dependent pathway and after its ubiquitination, it interacts with MFN2 and p62. PARKIN along with Ambra1 trigger these proteins to facilitate autophagy. In the case of parkin independent pathway, a different protein called the atg13 is phosphorylated upon interaction with ULK1, Cdc31 and

Hsp30. This causes Atg13 to induce both ROS activation and ATP depletion. mTOR which gets inhibited thereby prevents autophagy from taking place (Rakesh et al., 2022).

2.3.1.5. *Pexophagy*

Pexophagy has been reported to occur via two different pathways in mammals and yeast. Atg36, Pex3 and Atg30 bind with peroxisome in yeast and Hrr25 causes autophagy to be induced by activating increased expression of Atg36. The interaction of Atg11 and Atg8 with Atg36 results in the formation of pexophagosome after binding of the resulting complex with Pex11βp. However, the p62, NBR1 and SQSTM1 bind with the peroxisome. Pexophagosome is therefore formed when pex5 and ABCD1 proteins induce the interaction of peroxisomes with the Pex12, LC3II and Pex10 proteins (Rakesh et al., 2022).

2.3.1.6. *ER-phagy*

ER-phagy has been studied to occur through two different pathways in mammals and yeast. In mammals, autophagy can occur in three ways: in the tubular, various proteins are required for autophagy to occur such as the RTN3, CCPG1, and ATL3. When CNX binds with ATZ and FAM134B, ER derived vesicle is formed and this binds with VAMP8, leading to the formation of a phagosome. In the sheet of ER, the CCPG1, Sec62, FAM134B and TEX264 are required for autophagy to occur. In yeast however, ER-phagy requires the following proteins for autophagy formation: Lst1, Nvj1, Atg40, VAMP8, Sec23 and Atg39 (Rakesh et al., 2022).

2.3.2. Autophagy regulation

Autophagy is regulated in many ways and on its different system elements. In yeast, for example, the initiation and formation of phagosome components are controlled by the Atg1-Atg13-Atg17-Atg31-Atg29 kinase complex while in mammals, this same process is regulated by the Unc-51 like autophagy activating kinase 1 (ULK1). In addition to this, the kinase complex's regulatory function is further impacted when the main regulator of autophagy which is the mechanistic target of rapamycin complex 1 (MTORC1), interacts with it in close association. MTORC1's activation is fully dependent on the availability of nutrients in the cell (Tilija Pun et al., 2020).

When nutrients are present in a normal state, the interaction of MTORC1 with ULK1 and Atg13 which serve as the induction complex makes for their phosphorylation and inactivation. Therefore, the phagophore induction and autophagy formation are hindered. But when there is nutrient depletion due to increased metabolic demands or when deprivation of nutrient occurs in the cells, reduced signaling from the phosphoinositide3 kinase (PI3K)/Akt pathway and the Mitogen Activated Protein Kinase (MAPK) makes for the deactivation of MTORC1

and its subsequent release from its binding to the induction complex. Eventually, the induction complex is dephosphorylated and simultaneously activated. This therefore results into the activation of the downstream pathways of autophagy (Tilija Pun et al., 2020).

2.3.3. Autophagy and cancer

It has been reported that autophagy has the capacity to behave differently in different cell or pathological contexts as either a death inducing or cell survival path. This is sometimes referred to as the "autophagic paradox". Some are of the opinion that blocking autophagy flux can contribute to cancer death in some cancers and as such, the specific cause of a context specific behavior or role of autophagy must be investigated (Chmurska et al., 2021). For example, once the UV radiation resistance-associated gene (UVRAG) and Beclin 1 (BECN1) genes are mutated or other autophagy related genes such as ATG7, ATG3, and ATG5 are depleted, an increase in cell survival is of highest probability in various cancers (Rakesh et al., 2022). Several studies suggest that autophagy seems to have a suppressive role at the early stage of most cancer types, however, once a cancer has been established, it serves as a purveyor at its late stages- serving the cancer cell with its needs (Rakesh et al., 2022; Tilija Pun et al., 2020).

2.4. Micro RNA

MiRNAs are endogenously expressed small, single-stranded RNAs that are made up of about 21-25 nucleotides and function to regulate the expression of genes post-transcriptionally. They mostly bind to the 3' UTR of an mRNA target with a particular region called the seed region and thereby either inhibit the level of the gene's expression or maybe initiate its degradation. miRNA identification started with the discovery of the developmental regulator LIN-4 in Caenorhabditis elegans' developmental process. LIN-4 was found to be preserved amongst several organisms including in humans. This suggests a more general regulatory ability across different organisms. Over 30% of human genes could be regulated by miRNAs. MiRNAs can either regulate multiple targets or a group of miRNAs may be needed to regulate just one mRNA. That means they can each regulate more than one target individually or act collectively to regulate a single mRNA. This property of miRNAs implicates them in the regulation of several fundamental pathways in the body such as cell proliferation, cell cycle, and apoptosis. When the expression or activity of these miRNAs are disturbed in living systems, various disease outcomes are probable including neurodegenerative and cardiovascular diseases and cancer (Catani et al., 2021).

Other functions of miRNAs are still inconspicuous. To unravel how a gene works, typically, the gene is knocked down and the perceived changes before and after the knockdown are compared. But when you want to know how miRNAs work, we generally would not knock down its expression. Rather, we would either over-express it or limit its expression. MiRNA inhibitors are basically chemically arranged inhibitors with a specific targeting capacity for a specific miRNA. Once it hits its target, it lessens the endogenous amount of such miRNAs. It is also used in analyzing the impact of the loss of genes. MiRNA mimics and miRNA inhibitors have recently garnered so much keen attention for studying gene functions and providing new insights into drug clinical research and treatment (Zou et al., 2021). Figure 2.3 gives a schematic overview of how miRNAs work.

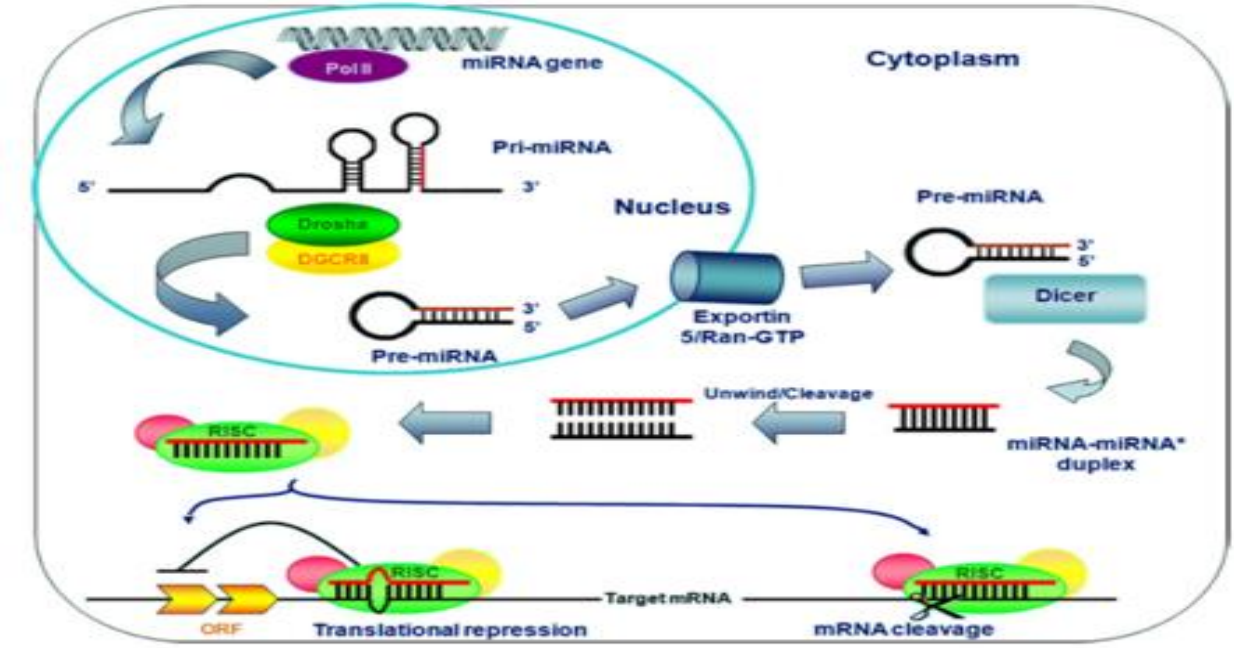

Figure 2.3. *Mechanism of microRNA action (Rani et al., 2022)*

2.4.1. Micro RNA biosynthesis

About half of the newly discovered miRNAs are intragenic and that means that they are usually transcribed from the introns and sometimes from the exons of genes that code for proteins. The rest of the miRNAs are intergenic and that means, they have their own genes and therefore they do not need a host gene to be transcribed. They have their own promoters and with these, they can be regulated. Also, some miRNAs are produced from genes as a single long transcript and these kinds of miRNAs are called clusters. They usually have similar seed regions and are mostly grouped as families (Rani et al., 2022).

MiRNA synthesis starts with the transcription of genes encoding the different miRNA types by RNA polymerase II. Only in certain conditions does RNA polymerase III play a similar role in transcribing miRNAs. The primary miRNA which is also known as the pri-miRNA is usually produced upon transcription in the nucleus and also takes up a double-stranded spiral shape. Drosha, an Rnase which is about 160kDa in weight and has an endonuclease activity act along with the factor DGCR8 (Di George Syndrome Critical Region Gene 8), and together they attach to the stem-loop structure of the pri-miRNA and afterward cut at a specific site to release a pre-miRNA. This process is known as cropping. Pre-miRNAs are usually 60-80 nucleotides long and they have a loop in their structure and a double-stranded stem which are complementary to each other and are made up of 33 nucleotide sequences. The pre-miRNA also has 2-3 nucleotides protruding at position 3' of their nucleotide sequence and also a phosphate group at position 5'. Once the pre-miRNA has been produced in the nucleus, it moves directly into the cytoplasm with the help of an exporter called the Exportin-5. In the cytoplasm, it continues its maturation process (Catani et al., 2021).

Once in the cytoplasm, an enzyme called the Dicer enzyme which is complexed with the TRBP (TAR RNA binding protein) attaches to the pre-miRNA and produces an 18-25 nucleotide long duplex RNA molecule. This miRNA duplex then activates two components to help direct it to recognize the mRNA target. RISC (RNA-Induced Silencing Complex) and the Argonaute 2 protein (AGO-2) are the two components. The two strands that make up the miRNA duplex have different fates. The thermodynamically less stable strand at the 5'-end position of the duplex is used as a guide strand which is complementary to the target messenger and facilitates its degradation (Catani et al., 2021).

If however, both stands at the 5' end-position have similar stability, any of the stands can therefore proceed to be the ripe miRNA. So, in naming each of these strands, a tag is added to tell from which of the filament was the miRNA formed. The miRNA formed is tagged with 3p if it was derived from the 3' precursors and 5p if it came to form the 5' precursors (Catani et al., 2021).

There are two pathways that lead to the biogenesis of miRNAs; the canonical and the noncanonical pathways. The canonical and non-canonical pathway of autophagy is represented in Figure 2.4.

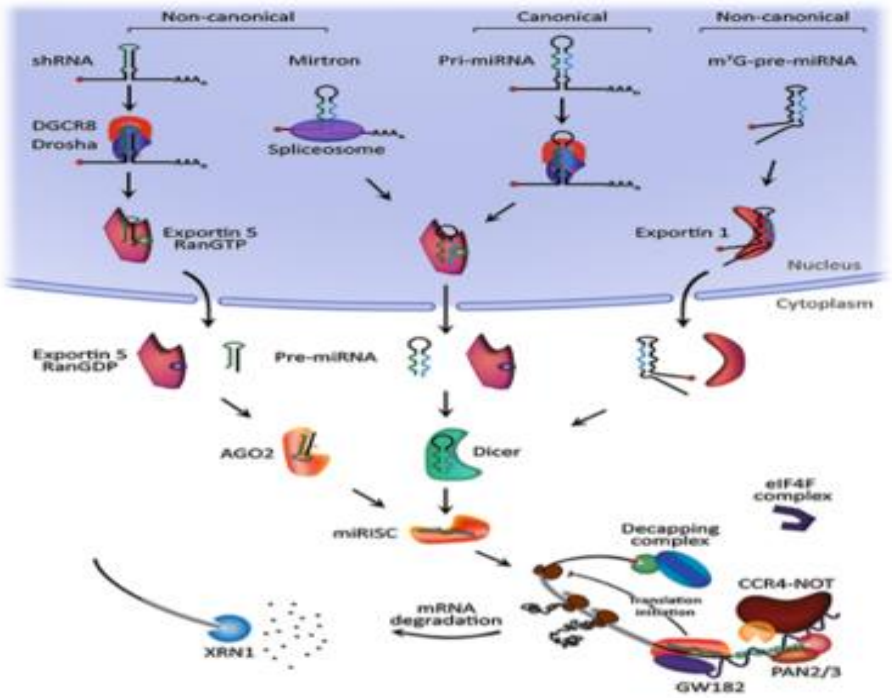

Figure 2.4. *Biosynthesis of miRNA (Rani et al., 2022)*

2.4.2. MicroRNA–mRNA interaction

MiRNAs target sites on mRNAs are not distributed evenly within the 3′ UTR, rather they are mostly grouped at both ends of 3′ UTR. In most cases, genes that have short 3′ UTRs tend to have their miRNA target sites located at the 5′ part of 3′ UTR. Different miRNAs could regulate alternative transcripts having varied 3′ UTR lengths. A lot of mRNAs host more than one target site for the same miRNA. When an mRNA has multiple sites, it provides the enhancement of the downregulation degree. Several target prediction algorithms are taking advantage of this property in their scans and scoring. There can be synergy between closely located target sites of the same or different miRNAs. Almost all the known miRNA-mRNA interaction in animals is characterized with the presence of bulges, strict complementarity areas and mismatches (Rani et al., 2022).

A region called the “seed” region is contained in each of the miRNA duplexes and it is found at the 5′ part of miRNA around the second to seventh position. It has a strict or nearly strict Watson–Crick pairing with its target site and is best conserved among miRNA sequences. It is worth noting that miRNAs are relatively heterogeneous and as such, no single model can be developed to explain the entire scope of their interaction with mRNAs (Rani et al., 2022).

MiRNA target sites on mRNAs may be classed into three according to the complementarity within the 5′ (the seed region) and 3′ area of the miRNA, namely: Canonical, 3′-compensatory and 3′-supplementary sites. Most of the known target sites are canonical. They typically possess a perfect pairing within the seed region that determines how certain the interaction is. Three types of the canonical sites have been discovered: The first is the 8mer that matches adenine in position 1 and 8. The second is 7mer1A with an adenine in the position 1 at the 5'end of miRNAs and the last type is the 7mer-m8 which matches in position 8. Most of the validated conserved target are mostly canonical sites. The 7mer sites are very much in place for very conserved miRNAs and the degree of gene silencing is improved upon by the adenine opposite position 1 of miRNA (Rani et al., 2022).

2.4.3. MiRNA and autophagy

The number of newly identified miRNAs is growing increasingly. Earlier, it has been reported that about 30 to 50% of protein-coding genes found in mammals have a regulatory impact by miRNAs. It has also been reported in various previous studies that miRNAs play some crucial roles in autophagy regulation. For example, miRNA-21 was reported to target rab11a in renal ischemia/reperfusion and therefore block autophagy. Both miRNA-16 and miRNA-15a have also been reported to promote Camptothecin-mediated sensitivity. MiR-21 is needed in the arsenite induction of autophagy. miRNA-199-3p, miRNA-99a, and miRNA-100 have been found to directly inhibit the growth and migration of tumor cells through their inhibitory influence on the 3′ UTR of mTOR. miRNA-155 is a major player in the progression of some diseases and in certain signaling paths' regulation such as autophagy, inflammation, and immunity. Autophagy is induced under hypoxia as miRNA-155 negatively regulates some of the mTOR signaling components e.g Rictor and Rheb (Zou et al., 2021).

Hundreds of the already discovered thousands of miRNAs have been linked with autophagy regulation. It was found that these miRNAs target genes of proteins that work in the different steps of the autophagy path. Also, some miRNAs have been found to target more than one of the genes that code for autophagy-related proteins. For example, several miRNAs have been found to target a central element required for regulating autophagy. miRNA100, miRNA 128, miRNA 338-3p, miRNA7, and miRNA96 have been described to target mTor. Even though we have talked about the regulation of autophagy by miRNAs, it is worth to also note that autophagy has a way of also regulating miRNAs. They have crosstalk and a mutual form of control over each other. Autophagy and autophagy-facilitated degradation is actively regu-

lating miRNAs and their machinery components. For example, miRNA 224 acting as an oncogene was selectively delivered for degradation in the lysosome. MiRNA18A has also been reported to be targeted by autophagy for degradation. In addition, elements in the miRNA maturation pathway such as DICER, DROSHA, and AGO have been discovered to be degraded by autophagy. It has also been discovered that free and miRNA-loaded AGO proteins are also degradable by autophagy. Therefore, there is some form of reciprocal connection between miRNA machinery and the autophagy pathway components. In this reciprocal control mechanism, we often find that a group of miRNAs act in concert to regulate the autophagy pathway but autophagy activity itself is enough to directly target miRNAs and their machinery components. This observation still needs to be elucidated for a clearer understanding (Akkoc & Gozuacik, 2020).

2.4.4. MiRNA use and application

The understanding of miRNA's functionality may be harnessed in creating new therapeutic options. Oncogenic miRNA activities may be inhibited with the help of miRNA inhibitors while the miRNA mimics may be employed to act instead of lost tumor suppressor microRNAs. Locked nucleic acids (LNA) antisense oligonucleotides (ASO) such as antagomirs and anti-mir oligonucleotides (AMO) can be used to block oncogenic miRNAs. MiRNAs activities may also be restored by introducing microRNAs coded by expression vectors or miRNA mimics (Szczepanek et al., 2022).

A number of anticancer therapies are currently harnessing the potential of tumor suppressor miRNAs. This approach is called miRNA replacement therapy and it involves the reactivation of pro-therapeutic pathways in cells after the introduction of these microRNAs. New therapeutic concepts now make use of miRNAs for the regulation of genes that are important for cancer progression. They are being used like the RNAi and antisense mRNAs to control cancer-related gene expressions. One of the key factors that drive cancer initiation is its high expression. Artificial miRNAs act based on their complementarity to the target mRNAs and thereby can be designed to block the expressions of selected oncogenes. It has been reported in a mouse study that when the miR-17-92 cluster is overexpressed, the c-Myc- induced apoptosis is strongly inhibited and this intensified the tumor development. The ability of this class of drugs to significantly repress the expression of target genes has been validated through clinical trials. Various antisense oligonucleotides with different nucleic acid analogs such as AMO, PNAs, and LNA, as well as nano-encapsulated PNAs may be used to silence miRNAs in vivo.

Other strategies for delivering anti-miRNAs and targeting are also in development (Szczepanek et al., 2022).

2.4.5. MiRNA and cancer

The screening for potential key targets of miRNAs is crucial for cancer research particularly because a single miRNA may control hundreds of target genes. One of the most intriguing areas of the many types of research currently in place is the identification of single or multiple sets of miRNAs with regulatory functions on the proliferation and death of cells. It has been reported that some miRNAs may negatively control the expression of oncoproteins in noncancerous cells and once their expression is affected, then it could result in the development and progression of cancer. microRNAs have been classed into 3 depending on what roles they play in cancer. Metastasis miRNAs that play some roles in metastasis, oncomiRs function as oncogenic miRNAs while we also have tumor suppressor miRNAs. If oncomiRs get over-expressed, then signatures of neoplastic diseases may be observed ranging from its initiation to its development or from its progression to its invasion. It is also challenging to classify miRNAs because many miRNAs may function as tumor suppressors and also play some roles in tumor development (Szczepanek et al., 2022).

Numerous studies have reported the essential roles of miRNA in cancer pathology. If the expression patterns of specific tumor cell phenotypes are identified, then cancers may be diagnosed and treated much earlier. Some studies have reported specific miRNAs expression patterns in leukemia, brain, breast, colorectal, and liver cancer. Once the signatures that are specific to miRNA activities are well understood, then these findings may be employed in the development of new therapies and prevention strategies for cancer. While miRNAs have been reported to be particularly involved in cancer pathology, the exact mechanism by which it regulates the many stages of cancer such as cancer initiation, metastasis, progression, and malignant conversion is still widely unclear. MiRNAs serve as good biomarkers because they are very stable and are easy to be identified in blood and other body fluids (Szczepanek et al., 2022).

2.4.6. MiRNA-155

MiRNA-155 can be found in the human chromosome 21q21.3. It was previously reported as an avian leucosis virus integration site. MiRNA-155 is hosted by mir155hg host gene. The mir155hg is also called the B-cell Integration Cluster (BIC) gene and it has three exons along a 13kb region which is situated in the human chromosome 21q21. It is transcribed to

produce the pri-miRNA-155 in exon 3 and pre-miRNA-155 is 1500bp in weight. It gets matured to produce the mature miRNA-155. Depending on how pri-miRNA-155 is processed, the mature sequence could either be designated as miRNA-155-5p or miRNA-155-3p. The first report that suggested that miRNA-155 has some roles to play in inflammation showed its high expression in B-cell lymphoma. MiRNA-155 is greatly conserved and has been reported to have some vital functions in mammalian immunity. It has been reported severally to be involved in the regulation of helper T cells' differentiation and also in helping to regulate macrophagic response through cytokine production (Catani et al., 2021; W. Chen et al., 2016).

MiRNA-155 plays a lot of functions in living systems. Initially, it was believed to be an immunomodulator and therefore act in several innate and adaptive immune responses. It is also functional in the regulation of numerous physiological processes such as apoptosis, cell proliferation, cell differentiation, and cell metabolism. It also plays some roles that are closely related to cancer. It was found that in patients with alcoholic liver and hepatitis C virus, miR-155 was greatly upregulated. It is active in the transforming growth factor-β-dependent epithelial-to-mesenchymal transition and growth of cells during hepatocarcinogenesis. It has been reported that miRNA-155, by targeting the rapamycin-insensitive companion of mammalian target of rapamycin (Rictor) and RAS homolog enriched in the brain (Rheb), in hypoxic conditions, regulates autophagy. MiRNA–155 has turned out to become a major regulator of the autophagy pathway. Furthermore, in alcoholic liver disease, miRNA-155 blocks the autophagy flux by targeting Lamp2 and Rheb/mTOR which leads to impaired lysosomal functionality (Zou et al., 2021).

MiRNA-155 has been reported to play huge roles in hematopoiesis, cardiovascular diseases, immunity, and inflammation. MiRNA-155 however, has a dual role in cancers either as an oncosuppressor-miRNA or an oncomiR depending on the context. MiRNA-155 has the ability to control cell survival, chemosensitivity, and growth upon FOXO3a targeting. It could also target VHL, RhoA signaling, and TGF-β signaling to promote tumor angiogenesis. It can also promote the proliferation of glioma through its regulation of MX11. SOCS1 is targeted by miRNA-155 in colon cancer and the invasiveness and tumorigenicity of colon cancers through the AKT and NF-kB pathways may be reduced once miRNA-155 is blocked. Furthermore, miRNA-155 has been found to be oncogenic (an oncomiR) in other cancer types such as oral squamous cell carcinoma, nasopharyngeal carcinoma, and pancreatic cancer. On the other hand, miRNA-155 has been found to suppress tumorigenesis in certain reports. For example, in melanoma, miRNA-155 was found to be proapoptotic and antiproliferative. The metastasis

of gastric cancer was weakened upon the downregulation of miRNA-155. Ovarian cancer-initiating cells (OCIC) adhesion and invasion are promoted by CLDN1. miRNA-155 can target CLDN1 but their expression is downregulated in these cancer cells. The drug resistance and apoptosis targets of miR-155 in ovarian cancers are, however, not completely known (W. Chen et al., 2016).

2.5. Hypoxia

Oxygen deficiency, a major hallmark of hypoxia in cells affects the function of cells. The past decade has been confronted with enormous efforts to elucidate the very complex process of hypoxia, how cells respond under a deprived oxygen state. A major highlight of these efforts which also serves as a breakthrough and impacted the world of physiology and disease is the discovery of Hypoxia-Inducible Factors (HIF) early in the 1990s (Ivan et al., 2022). Figure 2.5 gives a schematic representation of the hypoxia and normoxia signaling (Pereira et al., 2021).

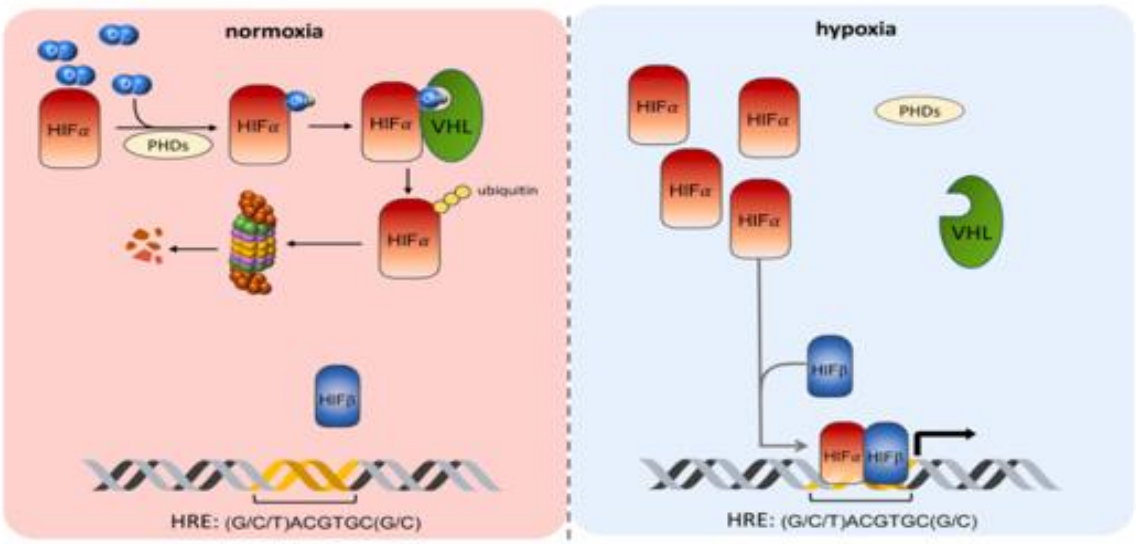

Figure 2.5. *Hypoxia signaling (Ivan et al., 2022)*

2.5.1. Hypoxia and ovarian cancer

HIF-1 is a heterodimer. It has HIF-1α as its regulatory part while the HIF-1β subunit is always expressed (constitutively). When hypoxia takes place in tissues, HIF-1α gets stabilized, accumulated, and moves to the nucleus. After it translocates to the nucleus, it activates genes that are sensitive to hypoxia or conserved hypoxia response elements such as VEGF through

its binding to their promoter region. HIF-1α and VEGF expressions are simultaneously increased in ovarian cells cultured under hypoxic conditions but if HIF-1a is inhibited, VEGF production and tumor angiogenesis are significantly decreased (Pereira et al., 2021).

More than 70% of human cancers including ovarian cancer has been shown to have an increased HIF-1α expression. So, HIF-1α is a major player in many ovarian cancer pathways. By acting as a transcription factor, HIF-1α promotes ovarian tumor development by regulating a spectrum of proteins. Many factors may influence the expression of HIF-1α in normal cells in the ovarian cancer microenvironment and this would also influence tumor cells characters. A lot of drugs have been developed based on the precision medicine concept to target tumor properties. One of these are the antiangiogenic agents with a major focus on VEGF, thereby helping address many pathophysiological states driven by VEGF to help lessen the burden of tumor patients such as those diagnosed with breast or ovarian cancer. Since VEGF operates below HIF-1α sequentially, the inhibition of HIF-1α leads to a concomitant reduction in VEGF expression. It is therefore promising to target HIF-1α for a reduction in tumor development (Wang et al., 2021) .

2.6. Camptothecin

Natural products are of great resource in the quest for new molecules that can help treat cancer. A lot of plant metabolite-derived compounds are frequently used in chemotherapy such as camptothecin, teniposide, and paclitaxel. The use of these drugs in clinical settings is however limited by their side effects on normal tissues and their ability to be easily resisted by cancer cells (Jin et al., 2017) .

Camptothecins are a group of compounds with close structures to the natural product Camptothecin (CPT). CPT was initially an extract of the Camptotheca acuminata tree which is native to southern china. A number of these family members have entered into clinical trials owing to their ability to inhibit topoisomerase I and serve as anti-cancer agents. Irinotecan which is a member of this family received approval for use by FDA in 1996 (D. Liang et al., 2018). Some studies have recently demonstrated that CPT and its derivatives have some potent anticancer effects in ovarian cancer, lung cancer, breast cancer and colorectal cancer both in vivo and invitro. CPT has been mechanistically studied to effectively induce cellular processes such as apoptosis, cell cycle progression etc. For example, CPT is able to stimulate mitotic arrest via Mad2-Cdc20 complex by JNK-facilitated Sp1 pathway activation. CPT has also been

shown to enhance cancer cell apoptosis using the miR-125b- mediated mitochondrial pathways to target the 3-UTR regions of p53, Bak1 and Mcl1 (Heng et al., 2021).

Top 1 hampers with DNA supercoiling. The anticancer effect of CPT is therefore established through transcription and replication interference which ultimately causes the cells to die from apoptosis. CPT is structurally composed of three fused rings namely pyrrolo-(3, 4-b)-quinoline part (rings A, B and C) which fuses with the pyridone (ring D) and thereby form a planar pentacyclic ring system. The active form of CPT has a chiral contained in a-hydroxy lactone ring (ring E) which has an (S)-configuration as described in Figure 2.6. (Swamy et al., 2021).

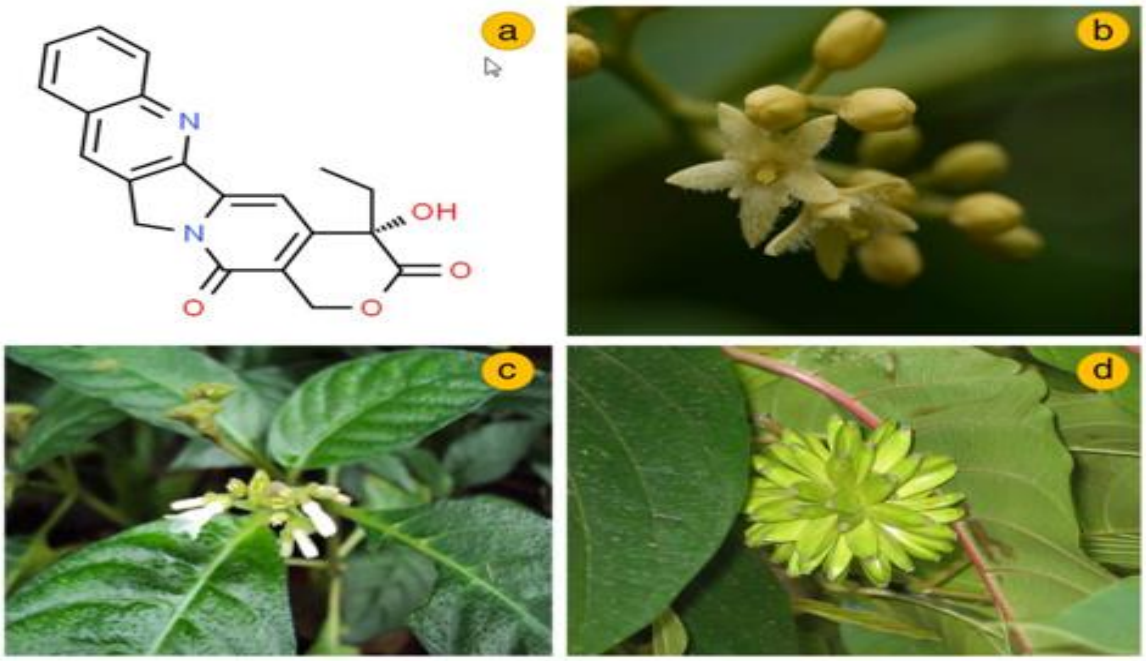

Figure 2.6. *Structure of Camptothecin ((Swamy et al., 2021)*

The wide spectrum application of CPT is not without limitations. CPT has a poor solubility in water. It is highly toxic to mammalian cells and rapidly hydrolyses the lactone ring *in vivo*. Furthermore, cells also acquire resistance against it (Swamy et al., 2021).

2.7. Chloroquine

The 4-aminoquinoline drug, CQ has found its use in many contexts ranging from malaria treatment to the treatment of rheumatoid arthritis (RA) and systemic lupus erythematosus (SLE) therapy. The potential of CQ in cancer and viral infection treatment was recently elucidated. It was shown to have some pleiotropic effects through complex mechanisms. CQ and its analogue HCQ both show high level of tolerance in humans, rapid onset, low toxicity and long duration of activity. When CQ gets metabolized in biological systems, it is partly converted to

monodesethyl metabolite and removed from the system mainly through the kidneys. CQ has a long half-life and as a result can be used once a week in the treatment of malaria. When an ethyl group in CQ is replaced by hydroxyl ethyl, HCQ is formed. This increases the distribution volume in humans and also lowers its toxicity (Zhou et al., 2020).

2.7.1. Chloroquine and autophagy

The use of CQ progressed from malaria treatment to the treatment of inflammations. CQ is able to increase the pH of cellular compartments as a result of its weak base character. So it was suggested that CQ increases the lysosomal pH and consequently block the autophagy flux since the hydrolases present in the lysosomes would be inhibited (Ovejero-Sánchez et al., 2021). Apart from its antimalarial effects, CQ exhibits promising therapeutic value in many cases such as in neurodegenerative diseases, autoimmune diseases, cardiovascular diseases and metabolic disorders through inhibition of toxins, prevention of inflammation and modification of melanin synthesis. The autophagy inhibition potentials of CQ and its tumor vascular normalisations credits CQ to be an anticancer adjuvant. It is able to suppress viral infection and replication as a result of its immunomodulatory and lysosomotropic properties. More studies should be embarked on in order to explain in more details, how CQ exactly causes this effect (Zhou et al., 2020).

3. MATERIALS AND METHODS

3.1. Cell Line

SKOV-3 (Human ovarian adenocarcinoma) cell line was obtained from the Biochemistry Research Laboratory of the Faculty of Pharmacy, Anadolu University.

3.2. Materials

3.2.1. Chemicals and consumables used

Table 3.1. *Chemicals and consumables used*

Name	**Company**
25 and 75 cm^2 cell culture flasks	Nest, China
24 and 96 well plates	Sarstedt, Germany
CIM-Plate	Roche, San Diego, CA
E-Plate	Roche, San Diego, CA
miRNA-155	Applied Biological Material Inc., BC, Canada
MTT Dye (Thiazolyl Blue Tetrazolium bromide)	Applichem, Germany
Dimethylsulfoxide (DMSO)	Sigma-Aldrich, Germany
Fetal Bovine Serum (FBS)	Sigma-Aldrich, Germany
Penicillin/Streptomycin	Sigma-Aldrich, Germany
Trypsin	Sigma-Aldrich, Germany
Dulbecco's modified eagle medium (DMEM)	Sigma-Aldrich, Germany
Ethyl alcohol	Detsan, Turkey
Opti-MEM	Gibco, USA
Camptothecin	Sigma-Aldrich, Germany
Chloroquine	Sigma-Aldrich, Germany

3.2.2. Equipment

Table 3.2. *Equipment*

Equipment	Company

Sterile CO_2 incubator	Hera Cell 240 Thermo Scientific, Germany
Autoclave	ALP, Japan
Refrigerated centrifuge	Heraheus, Germany
Fluorescent microscope	Leica DMI 4000B, Germany
Nitrogen tank	Taylor Wharton, Germany
Refrigerator	Arcelik, Turkey
Deep freezer (-20°C)	Arcelik No Frost, Turkey
Distilled water device	Nuve, Turkey
Precision balance	Ohaus, Switzerland
Inverted microscope	Leica, Germany
Laminar cabin	HealForce, China
Sterilizer	Nuve FN 500, Turkey
Water bath	Nuve BM 302, Turkey
Vortex	Yellowline, Belgium
DNA/RNA UV cabinet UVT-B-AR	Biosan, Turkey
xCELLIGENCE Real Time Cell Analysis system	Roche, Germany
Freezer (-80°C)	New Brunswick Scientific, USA
Oven	Nuve, Turkey
Shaker	Biometra WT17, Germany
Enzyme-linked immunosorbent method reader (ELISA)	BioTek Elx800, US
pH meter	Thermo Scientific, Singapore

3.2.3. Commercial kits used

Table 3.3. *Commercial kits used*

Name	**Company**
Lipofectamine RNAiMAX transfection kit	Invitrogen, USA
Autophagy Assay Kit	Sigma-Aldrich, USA

3.2.4. Computer programs used

Table 3.4. *Computer programs used*

Name	Company
Graphpad Prism 9	USA
RTCA Software 2.0	Roche, Germany
BioTek Gen5 Data Analysis Software	BioTek, US
FIJI-Image J	Open source

3.3. Preparation of Used Materials

3.3.1. Dissolution and preparation of Camptothecin and Chloroquine

CPT and CQ were each weighed separately on a precision balance. CPT was weighed for 2 mg while CQ was weighed for 1 mg. The 2 mg of CPT was dissolved in 1ml of pure DMSO (dimethylsulfoxide) while the 1 mg of weighed CQ was dissolved in 3.877 ml of distilled water.

For the determination of the effective concentration, CPT and CQ were prepared in DMEM medium containing 10% FBS. Concentrations of 2.5-30 μM/ml CQ and 2-70 μg/ml CPT were prepared separately and used in DMEM medium with 10% FBS.

3.3.2. Preparation of miRNA-155 mimic, miRNA-155 mimic inhibitor and their negative controls

To make a 100 μM stock solution of the miRNA-155 miRNA mimic, 25 μL of nuclease-free water was added to re-suspend the lyophilized synthetic miRNA-155 mimic (2.5 nmol) and the solution was mixed briefly in vortex to ensure a smooth mixture as recommended in the product datasheet of the mimic.

To make a 100 μM stock solution of the miRNA-155 miRNA inhibitor, 50 μL of nuclease-free water was added to re-suspend the lyophilized synthetic miRNA-155 inhibitor (5 nmol) and the solution was mixed briefly in vortex to ensure a smooth mixture as recommended in the product datasheet of the mimic.

To make a 100 μM stock solution of the miRNA Mimic Negative Control, 25μL of nuclease-free water was added to re-suspend the lyophilized synthetic miRNA Mimic Negative

Control (2.5 nmol) and the solution was mixed briefly in vortex to ensure a smooth mixture as recommended in the product datasheet of the mimic.

To make a 100 μM stock solution of the miRNA inhibitor Negative Control, 50 μL of nuclease-free water was added to re-suspend the lyophilized synthetic miRNA inhibitor Negative Control (5 nmol) and the solution was mixed briefly in vortex to ensure a smooth mixture as recommended in the product datasheet of the mimic.

100 nM concentration of all these synthetic miRNAs was used in the experiments contained in this study. Since the synthetic miRNAs can be frozen and thawed up to 3 times, aliquots were made with 2.5 μL of the prepared miRNA-155 miRNA mimic solution, 5 μL of the prepared miRNA-155 miRNA inhibitor solution, 2.5 μL of the prepared miRNA Mimic Negative Control solution and 5 μL of the prepared miRNA inhibitor Negative Control solution in different tubes, for ease of use. Prepared eppendorf tubes were stored at -20°C.

3.3.3. Cell culture

3.3.3.1. *Normoxia treatment*

SKOV-3 cells were kept in culture medium at 37 °C in a DMEM medium containing 10% fetal bovine serum, 1% penicillin-streptomycin, 1% L-glutamine in a 5% CO_2 incubator and proliferated. At 80% confluence (~2-3 days), the cells were sub-cultured with 1× trypsin solution at a ratio of 1:3 to 1:6 and the cells were grown.

3.3.3.2. *Hypoxia treatment*

SKOV-3 cells were kept in culture medium at 37 °C in a DMEM medium containing 10% fetal bovine serum, 1% penicillin-streptomycin, 1% L-glutamine in a hypoxia incubator (1% oxygen levels and 5% CO_2) and proliferated. At 80% confluence (~2-3 days), the cells were sub-cultured with 1× trypsin solution at a ratio of 1:3 to 1:6 and the cells were grown.

3.3.4. Cytotoxicity detection test

3.3.4.1. *Determination of the IC_{50} dose of Chloroquine and Camptothecin by MTT assay*

The MTT method is a method used most commonly to determine cell viability, cell proliferation and cytotoxicity. In this assay, cells with active mitochondrial function, convert the tetrazolium ring in MTT (3-4,5-dimethylthiaol-2)-2, -5 diphenyltetrazolium bromide) dye

to formazan by the mitochondrial dehydrogenase enzyme and living cells are able to give a purple color change.

Conversely, dead cells with inactive mitochondria are unable to produce a colour change since they have lost their mitochondrial reduction function.

Cells were seeded in 96-well plates at 1×10^4 cells per well and incubated for 24 hours. At the end of 24 hours, the nutrient medium was changed and CQ and CPT were applied to the cells in separate plates in a concentration range of 2.5-30 μM/ml for 24 and 48 hours for CQ and in a concentration range of 2-70 μg/ml for 24 and 48 hours for CPT. At the end of the incubation times, 20 μl of MTT dye was added to each well and left to incubate for 4 hours. At the end of the incubation period, the medium was removed and 200 μL of DMSO was added to dissolve the formed formazan crystals. Plates were mixed on a linear shaker for approximately 10-15 minutes in the dark. Finally, the absorbance of the colour emitted by the cells was read at a wavelength of 490 nm on the spectrophotometric microplate reader. The absorbance value showing 50% inhibition of cells was considered the IC_{50} value and was calculated using Graphpad Prism 9 software.

3.3.5. Transfection of mimic, mimic inhibitor and their negative controls

MiRNA-155 mimic, miRNA-155 inhibitor, miRNA-155 mimic negative control and miRNA-155 inhibitor negative control are synthetic molecules designed to mimic the endogenous miRNA molecular functions. 96-well plates were used for transfection. 1×10^4 cells were first plated and incubated for 24 hours. Since cells reached 60-80% density after 24 hours and in separate wells, MiRNA-155 mimic, miRNA-155 inhibitor, miRNA-155 mimic negative control, and miRNA-155 inhibitor negative control were transfected.

The Lipofectamine RNAiMAX Transfection Kit (Invitrogen, USA) was used for transfection. Two separate eppendorf tubes were taken and Lipofectamine RNAiMAX was diluted in Opti-MEM medium in accordance with the kit procedure in one, while MiRNA-155 mimic, miRNA-155 inhibitor, miRNA-155 mimic negative control and miRNA-155 inhibitor negative control were diluted in Opti-MEM medium in another separate tubes.

Afterwards, the mixture of Opti-MEM and the individual miRNA molecules was separately mixed with the lipofectamine RNAiMAX mix and incubated for 5 minutes at room

temperature. Subsequently, the miRNA-lipid complex was added to the cells and incubated for different time points and subjected to further treatments depending on what is to be determined.

3.3.6. Quantitative determination of cell proliferation by xCELLigence real time cell analysis (RTCA)

Using the RTCA device, the proliferation of SKOV-3 ovarian cancer cells transfected in the presence or absence of CQ, CPT and miRNA-155 mimic and miRNA-155 negative inhibitor was quantitatively evaluated using E-plates. E plates were first filled with medium and placed in the RTCA device to measure the background and ensure that the plates are in good condition for the experiment. After these has been confirmed, $1x10^4$ SKOV-3 cells were plated on these plates in DMEM medium containing 10% FBS and left to incubate for 24 hours. After 24 hours of incubation, the media with was removed and replaced with serum-free and antibiotic-free media and the cells were transfected with miRNA-155 mimic, miRNA -155 inhibitor and their negative controls as described in section 3.3.4., following the instructions in the Lipofectamine RNAiMAX transfection kit.

After the first 48 hours of the experiment, CQ concentrations of 10.2 μM/ml (IC_{50}) and CPT concentrations of 3.5 μg/ml (IC_{50}) were added to separate cell groups and the cells were incubated for another 72 hours to make a total of 120 experimental hours.
The RTCA device was used to document changes in the proliferation of these cells by measuring the cell index under the above-mentioned treatments and in real-time. After the experiment, the morphology of the cell**s** was observed under a light microscope, and the cell images under the light microscope were taken.

3.3.7. Quantitative determination of cell migration by xCELLigence real time cell analysis (RTCA)

This experiment was done using the xCELLigence real-time cell analysis (RTCA) instrument. With the RTCA device, real-time analysis of cell-based tests such as migration, proliferation and cytotoxicity is performed with extremely sensitive impedance technology in cell culture environments. The migratory ability of miRNA-155 transfected into SKOV-3 cells in the presence or absence of CQ, CPT and miRNA-155 negative inhibitor was quantitatively evaluated. The whole set up was done in the incubator to obtain a continuous and real-time map of the response of the SKOV-3 cells to different treatments. CIM plates were first filled

with medium and placed in the RTCA device to measure the background and ensure that the plates are in good condition for the experiment. After these has been confirmed, $1x10^4$ SKOV-3 cells were plated on these CIM plates in DMEM medium containing 10% FBS and left to incubate for 24 hours. After 24 hours of incubation, the media with was removed and replaced with serum-free and antibiotic-free media and the cells were transfected with miRNA-155 mimic, miRNA-155 inhibitor and their negative controls as described in section 3.3.4., following the instructions in the Lipofectamine RNAiMAX transfection kit.

After the first 48 hours of the experiment, CQ concentrations of 10.2 μM/ml) and CPT concentrations of 3.5 μg/ml (IC_{50}) were added to separate cell groups and the cells were incubated for another 48 hours.
The RTCA device was used to document changes in the migration of these cells under the above mentioned treatments.

3.3.8. Determination of autophagy flux

The autophagy assay kit was used to measure the level of autophagy in SKOV-3 ovarian cancer cells transfected with miRNA-155, miRNA -155 inhibitor and their negative controls. These transfected cells were further treated with either CPT the autophagy inducer or CQ the autophagy inhibitor. The set-up was done under both normoxia and hypoxia. This method helps to understand and give some information about how miRNA-155 affects the autophagy pathway.

SKOV-3 ovarian cancer cells were transfected with 100 nM miRNA-155 mimic, miRNA-155 inhibitor, miRNA-155 mimic negative control and miRNA-155 inhibitor negative control using the Lipofectamine RNAiMax transfection kit as described in section 3.3.4. After the first 48 hours of the experiment, the cells were later treated with CQ 10.2 μM/ml (IC_{50}) and CPT 3.5 μg/ml (IC_{50}) separately to the different experimental groups. At the end of the incubation period an autophagy detection reagent solution was prepared by diluting 20μL of the 500 × solution with 10 ml of the stain buffer. The medium on the incubated cells was removed and 100 μL of the Autophagosome detection reagent working solution was added to each well and incubated for 1 hour. The cells in each well were later washed 3-4 times with 100 μL of wash buffer supplied in the kit. The buffer was removed and the fluorescence intensity was

measured using a fluorescence microscope with a FITC filter at 40× magnification. The autophagic vacuole is represented by the green particles in autophagic cells.

3.3.9. Statistical analysis

Statistical analysis was performed on the Graphpad Prism 9.0 software using one-way ANOVA with Benferroni's post hoc tests for differences between more than two groups and the two-tailed Student T-test for differences between two groups. The results of at least two independent replicates were expressed as mean ± standard mean error (SEM), and p values less than 0.05 were considered statistically significant.

4. RESULTS

4.1. Cytotoxicity Results

4.1.1. Cytotoxic effect of Chloroquine on SKOV-3 cancer cells

In this experiment, $1x10^4$ SKOV-3 cells were plated and incubated with different concentrations of CQ (2.5, 5, 7.5, 10, 20, 30 μM) for different time points. For each incubation time point completion, MTT dye was added to the cell medium and incubated at 37°C for 4 hours. The formazan salts formed by the cells after the incubation was dissolved with DMSO and the intensity of the color change was detected at a wavelength of 490 nm for each well on the ELISA Reader device. Cell viability was calculated by normalizing the control cell group to 100%. The IC_{50} values of CQ at different time points were determined with the Graphpad Prism9 software. Three independent experiments were performed in this study with at least 3 replicates (n>=3) in each individual experiment. The statistical difference with the control group was analyzed with one-way ANOVA. The observe value of CQ at 48 hours is shown in Table 4.1. The percent % viability values of SKOV-3 cells exposed to CQ for 48 hours were calculated and the statistical difference compared with the control group is shown in the graphs in Figure 4.1.1.

Table 4.1. *IC_{50} values of Chloroquine and Camptothecin in SKOV-3 cell line at 48 hours*

Compound	**Hours**	**IC_{50}**
Chloroquine	48 hours	10.2 μM
Camptothecin	48 hours	3.5 μg/ml

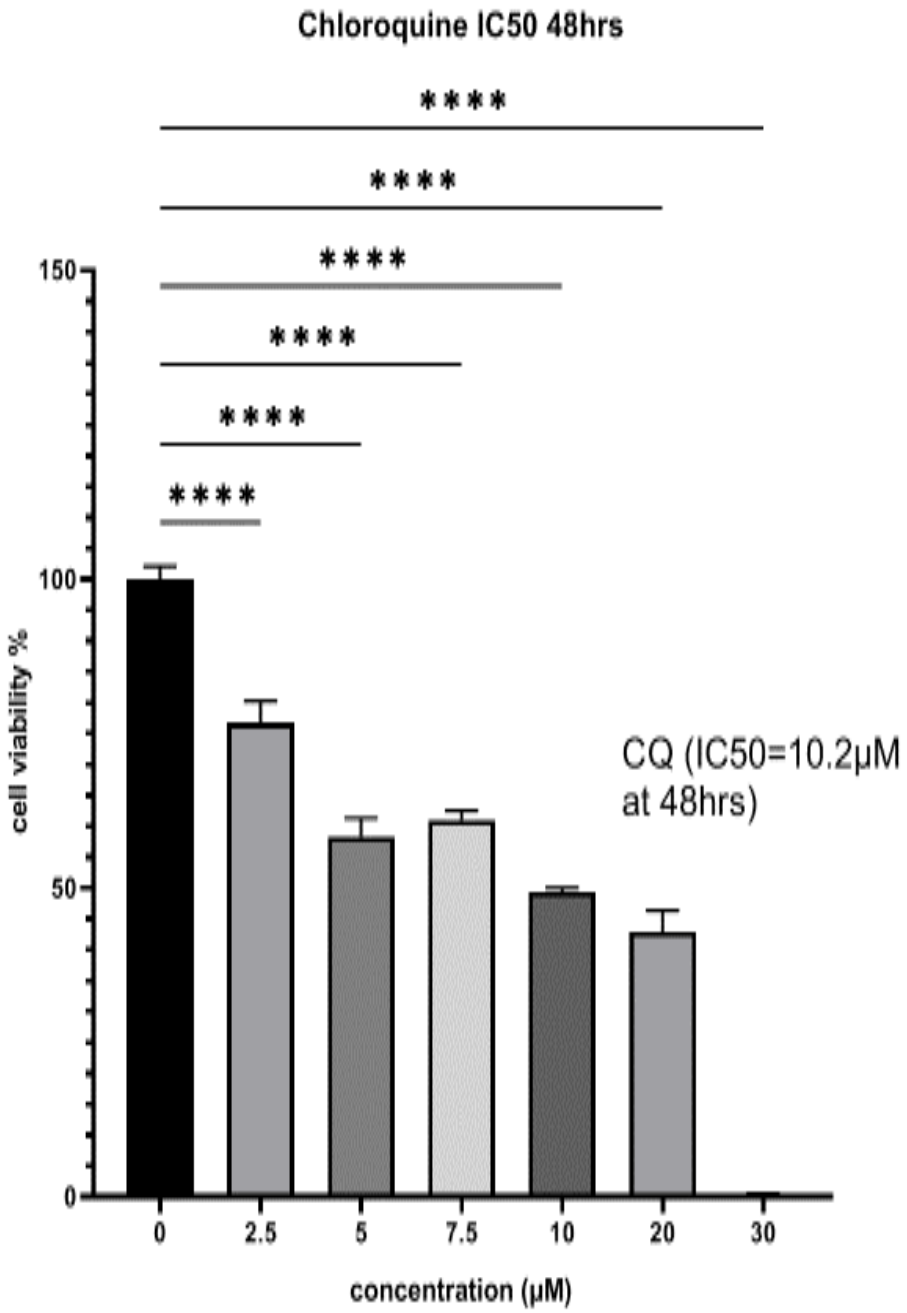

Figure 4.1.1. *Cell Viability (%) of Chloroquine after 48 hours incubation in SKOV-3 cells by MTT assay. Viability data are mean ± SEM. (n≥3) at each time slot and in each concentration group. Analysis with one-way Anova ** $p < 0.05$ *** $p < 0.001$ **** $p < 0.0001$. The graph shows the mean of three independent experiments*

In the MTT test, as a result of the exposure of SKOV-3 cells to CQ for 48 hours, the cell viability values showed a significant dose-dependent decrease. Cell viability was found to start dropping below 50% over a 48hour period with CQ concentrations ≥10 μM. A sharp decrease in cell viability was observed from 20 to 30 μM. Our unreported data with concentration ranges from 50 to 100 μM of CQ did not show any cell viability after 48 hours of incubation (Figure 4.1.1).

After incubation of SKOV-3 ovarian cancer cells with CQ for 48 hours, the IC_{50} concentration on SKOV-3 cells was found to be 10.2 μM (Table 4.1.1). In comparison with the control group, a statistically significant decrease was determined at all concentrations ($p<0.05$).

4.1.2. Cytotoxic effect of camptothecin on SKOV-3 cancer cells

In this experiment, $1x10^4$ SKOV-3 cells were plated and incubated with different concentrations of CPT (2, 5, 8, 10, 20, 30, 40, 50, 60, and 70 μg/ml) for different time points. For each incubation time point completion, MTT dye was added to the cell medium and incubated at 37°C for 4 hours. The formazan salts formed by the cells after the incubation was dissolved with DMSO and the intensity of the color change was detected at a wavelength of 490 nm for each well on the ELISA Reader device. Cell viability was calculated by normalizing the control cell group to 100%. The IC_{50} values of CPT at different time points were determined with the Graphpad Prism9 software. Three independent experiments were performed in this study with at least 3 replicates ($n\geq3$) in each individual experiment. The statistical difference with the control group was analyzed with one-way ANOVA. The observed IC_{50} value of CPT at 48 hours is shown in Table 4.1. The percent % viability values of SKOV-3 cells exposed to CPT for 48 hours were calculated and the statistical difference compared with the control group is shown in the graphs in Figure 4.1.2.

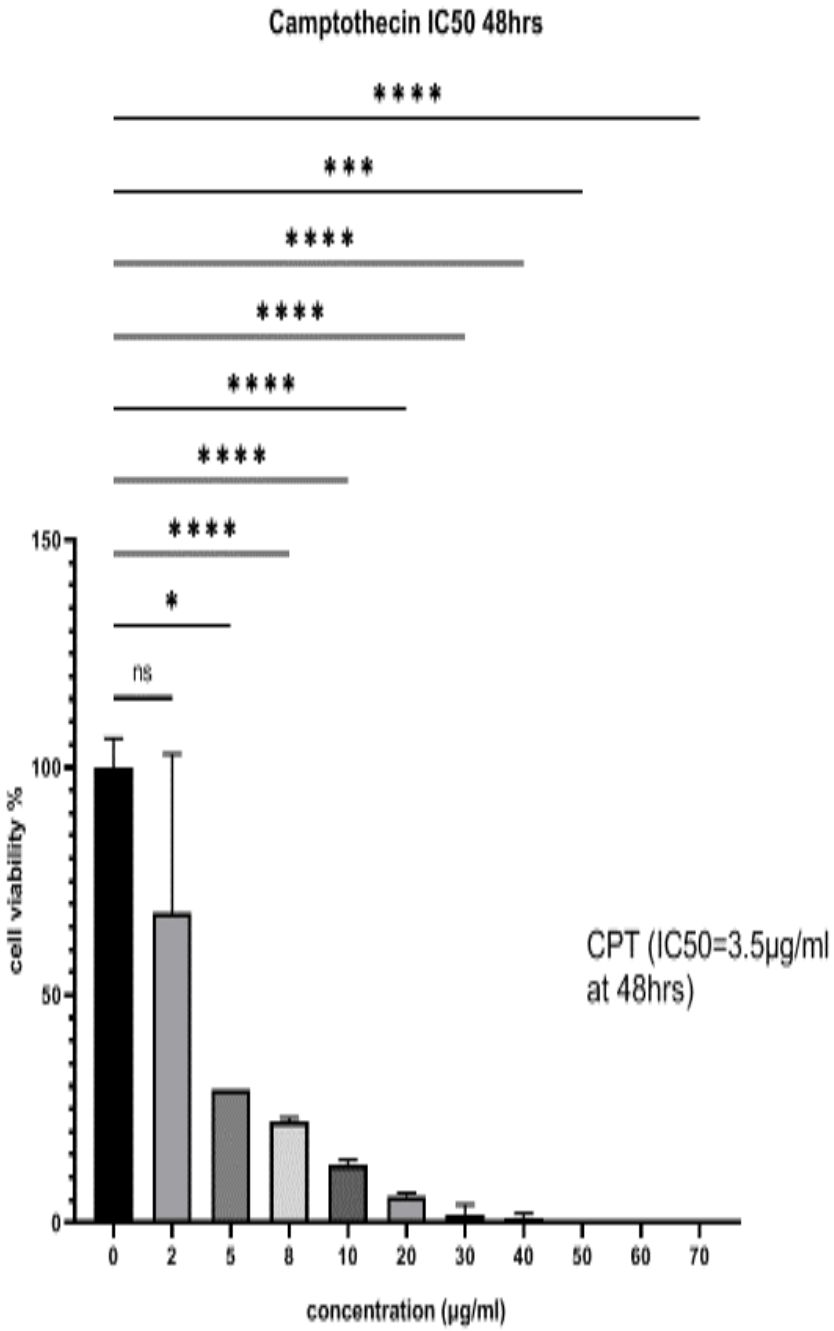

Figure 4.1.2. *Cell Viability (%) of Camptothecin after 48 hours incubation in SKOV-3 cells by MTT assay. Viability data are mean ± SEM. (n>=3) at each time slot and in each concentration group. Analysis with one-way Anova ** p < 0.05 *** p < 0.001 **** p < 0.0001. The graph shows the mean of three independent experiments*

In the MTT test, as a result of the exposure of SKOV-3 cells to CPT for 48 hours, the cell viability values showed a significant dose-dependent decrease. Cell viability was found to start dropping below 50% over a 48-hour period with CPT concentrations ≥ 2µg/ml. A sharp decrease in cell viability was observed from 2 to 5 µg/ml. Concentration ranges from 8 to 70 µg/ml of CPT showed less than 15-0% cell viability after 48 hours of incubation (Figure 4.1.2).

After incubation of SKOV-3 ovarian cancer cells with CPT for 48 hours, the IC_{50} concentration on SKOV-3 cells was found to be 3.5 µg/ml (Table 4.1.1). In comparison with the control group, a statistically significant decrease was determined at all concentrations ($p<0.05$).

4.2. Transfection Results

4.2.1. Effect of miR-155 miRNA mimic transfection on SKOV-3 ovarian cancer cells

SKOV-3 ovarian cancer cells were incubated for 24 hours after seeding into E-plates. After incubation, 3 different concentrations (50 nM, 100 nM, and 200 nM) of miRNA-155 mimic, miRNA-155 inhibitor, and their respective negative controls were prepared separately and the Lipofectamine RNAiMax transfection kit was used to transfect them into SKOV-3 ovarian cancer cells after 24 hours of plating. The cells were incubated for another 72 hours and the cell index was measured using the RTCA device.

The graphical results of the changes in the cell index of miRNA-155 mimic, miRNA-155 inhibitor, and their respective negative controls at different concentrations are shown in Figures 4.2.1 and 4.2.2.

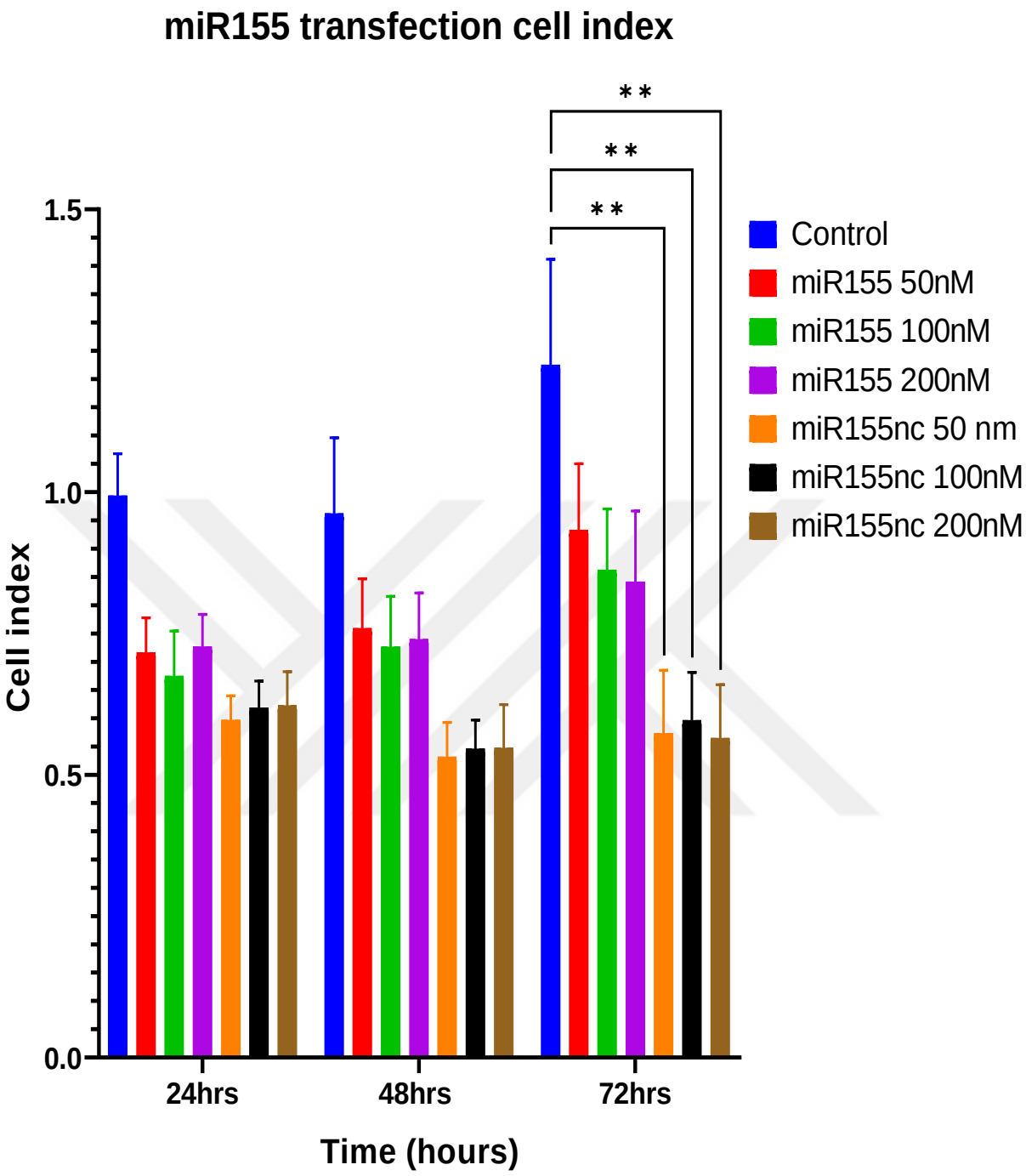

Figure 4.2.1. *Transfection of SKOV-3 cells with different concentrations of miR-155 miRNA mimic and its negative control. Cell index data are mean ± SEM of three independent experiments with n=6. Analysis with two-way Anova ** $p < 0.05$ *** $p < 0.001$ **** $p < 0.0001$. The graph shows the mean of three independent experiments*

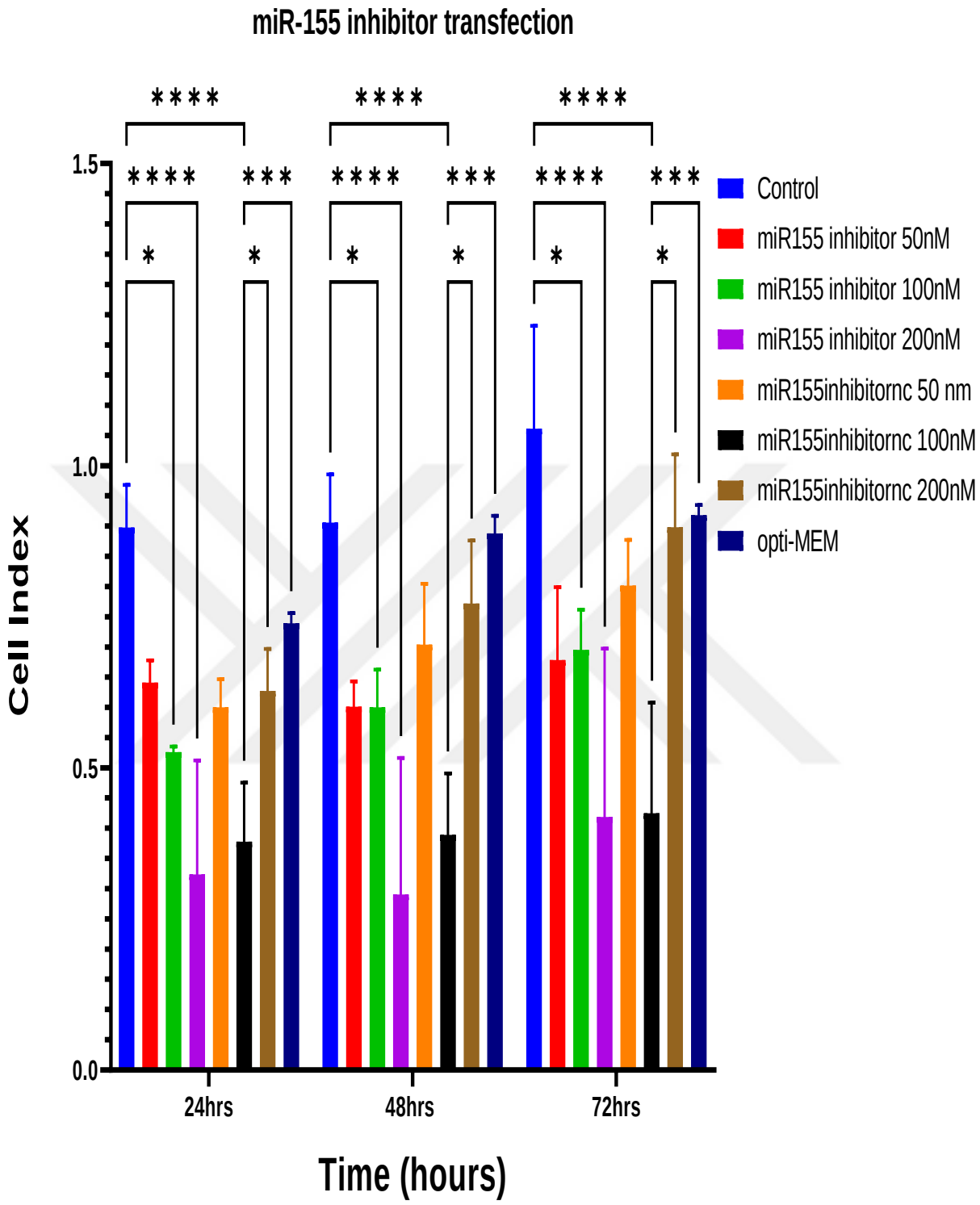

Figure 4.2.2. *Transfection of SKOV-3 cells with different concentrations of miR-155 miRNA inhibitor and its negative control. Cell index data are mean ± SEM of three independent experiments with n=6. Analysis with two-way Anova ** $p < 0.05$ *** $p < 0.001$ **** $p < 0.0001$. The graph shows the mean of three independent experiments*

The results of the proliferation confirmed the opposite effect of both the miRNA-155 miRNA mimic and its inhibitor upon transfection into SKOV-3 ovarian cancer cells. While a significant change in cell index was not observed with the transfection of the miRNA-155 miRNA mimic into SKOV-3 ovarian cancer cells, a significant difference in comparison with the untransfected control group was observed in the cell index profile of SKOV-3 ovarian cancer cells transfected with miRNA-155 miRNA inhibitor. The cell index particularly at 100 nM and 200 nM significantly decreased with the miRNA-155 miRNA inhibitor for all time points. Conversely, the inhibitor negative controls showed opposite effects.

Consequently, to this noticeable observed opposite differences in the transfection results which suggests that the inhibitor significantly decreased the cell index of SKOV-3 cells, for subsequent studies, 100 nM concentration of both the mimic, its inhibitor, and their respective negative controls was selected as the concentration to be used for subsequent experiments in this study.

4.2.2. Effect of Chloroquine and Camptothecin on the proliferation of SKOV-3 ovarian cancer cells transfected with miRNA-155 miRNA mimic and miRNA-155 miRNA inhibitor in normoxia and hypoxia

SKOV-3 ovarian cancer cell line was seeded on E-plate and incubated in the RTCA system for 24 hours to ensure cell attachment either in a normoxia or hypoxia incubator. At the end of the incubation period, cells were separately transfected with 100 nM miRNA-155 miRNA mimic, 100 nM miRNA-155 miRNA inhibitor, and 100 nM each of their negative controls. After 24 hours of transfection, the transfection media was removed and replaced with a medium containing either CQ (10.2 μM) or CPT (3.5 μg/ml), and the cells were left to incubate for 72 more hours. The CI values were measured in RTCA throughout the whole experiment. The analysis results of the experiment were normalized according to the time CQ or CPT was added in the RTCA software program and the CI values were determined. No transfection or inhibitor application was made to the cells in the control group. Cell proliferation rates were calculated from the CI values obtained at the different time points, and compared to the control group. The results are given in two independent experiments with n=4. These are shown in figure 4.2.3 to Figure 4.2.6.

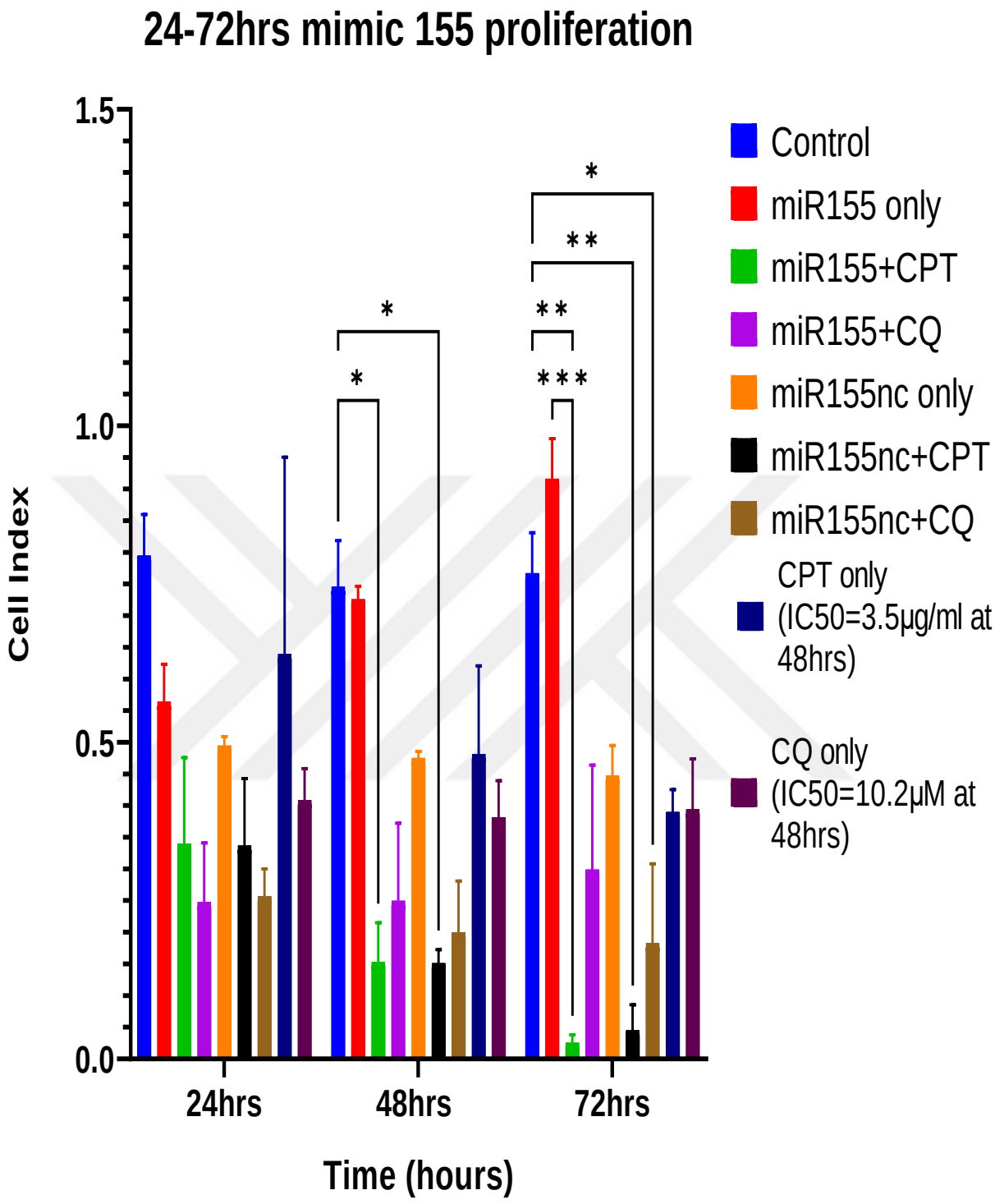

Figure 4.2.3. *Effect of Chloroquine and Camptothecin on the proliferation of SKOV-3 ovarian cancer cells transfected with miR-155 miRNA mimic and negative control in normoxia. Cell index data are mean ± SEM of three independent experiments with n=6. Analysis with two-way Anova ** $p < 0.05$ *** $p < 0.001$ **** $p < 0.0001$. The graph shows the mean of three independent experiments*

The data obtained from the RTCA software program for the different treatment groups was used to plot the graph of time against the cell index.

As seen in Figure 4.2.3, 24 hours after CQ or CPT treatment of SKOV-3 ovarian cancer cells transfected with miRNA-155 miRNA mimic or its negative control in normoxic conditions, there were no significant differences in the proliferation levels of the control groups and the individual treatment groups. After 48 hours of further incubation of miRNA-155 miRNA mimic or its negative control transfected SKOV-3 cells treated with CPT, a statistically significant difference was observed in the cell index level of the untransfected SKOV-3 cells and the cells transfected with miRNA-155 miRNA mimic and 24 hours later treated with CPT for 48 hours. This decrease was also observed between the control group and the group transfected with the negative control and treated with CPT. This suggests that CPT decreases the proliferation rate of cells transfected with both the miRNA-155 miRNA mimic and its negative control. 72 hours of further incubation of miRNA-155 miRNA mimic or its negative control transfected SKOV-3 cells in normoxic conditions and treated with either CQ or CPT, showed some statistically significant differences. Statistical difference was observed in the cell index level of the SKOV-3 cells transfected with the group transfected with miRNA-155 miRNA mimic only and the group transfected with miRNA-155 miRNA mimic and 24 hours later treated with CPT for 72 hours. This same statistical difference was observed in the cell index levels of the control group and the group transfected with miRNA-155 miRNA mimic and 24 hours later treated with CPT for 72 hours. A statistically significant decrease was also observed between the group transfected with miRNA-155 miRNA mimic only and the group transfected with miRNA-155 miRNA mimic and 24 hours later treated with CQ for 72 hours.

A statistically significant decrease was observed between the untransfected group (control group) and the group transfected with the mimic negative control and 24 hours later treated with either CQ or CPT for 72 hours. These data suggest that the combinatory treatment of miRNA-155 miRNA mimic and CPT greatly reduces the proliferation rate of SKOV-3 ovarian cancer cells in comparison with the untransfected control group, miRNA-155 miRNA mimics only transfected group and the CPT only treated group. Interestingly, while the proliferation rate of the control group remained similar across the three-time points of observation (24, 48, and 73 hours post incubation with drugs), the miRNA-155 miRNA mimic transfected SKOV-3 ovarian cancer cells had an increased proliferation rate as time passed. This suggests that the miRNA-155 miRNA mimic may increase the proliferation rate with time. Similarly, the negative control-only transfected group had no obvious changes in its cell index or proliferation rate

as time passed. This confirms the inability of this miRNA to induce a possible effect as compared to the mimic.

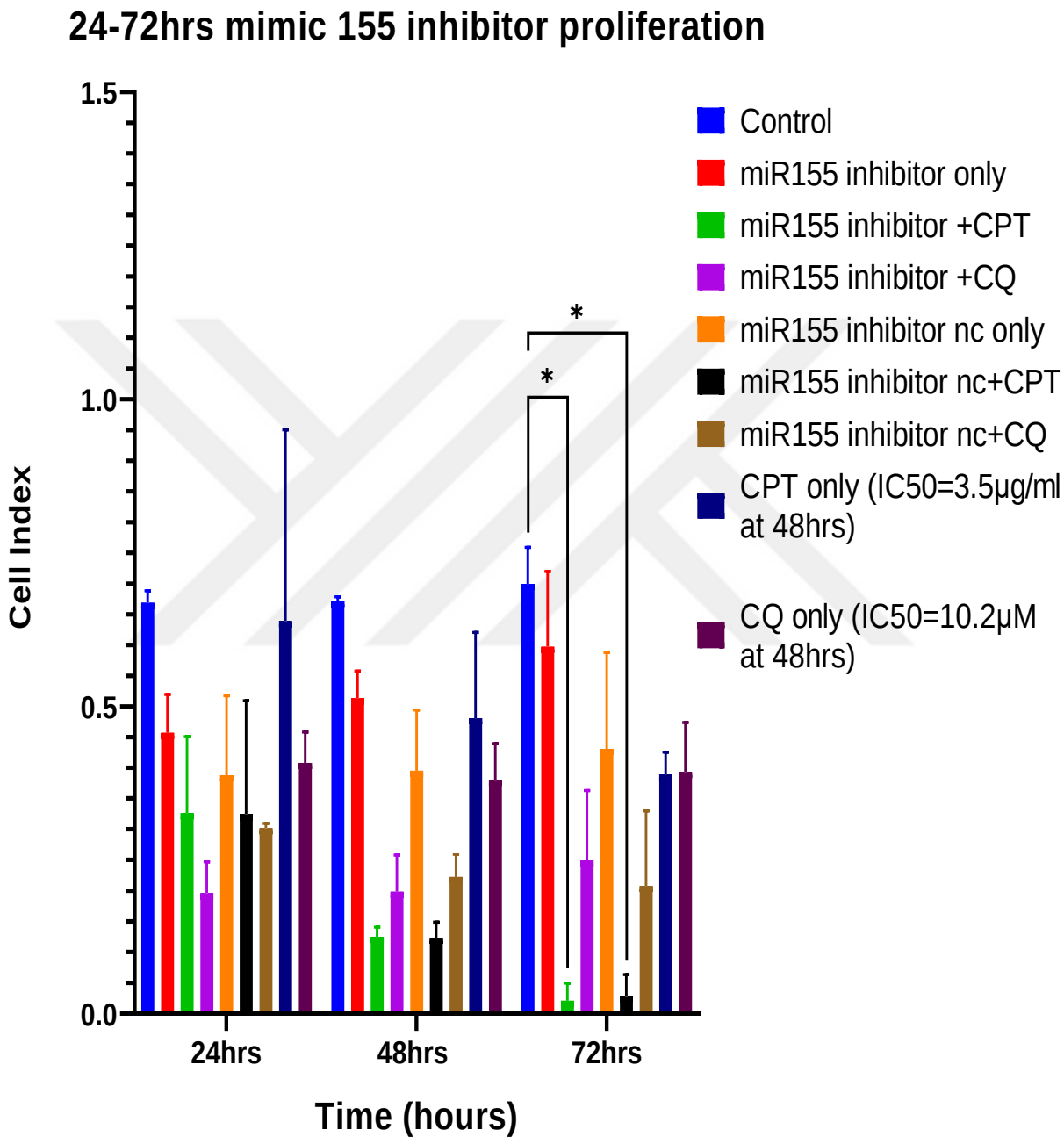

Figure 4.2.4. *Effect of Chloroquine and Camptothecin on the proliferation of SKOV-3 ovarian cancer cells transfected with miR-155 miRNA inhibitor and negative control in normoxia. Cell index data are mean ± SEM of three independent experiments with n=6. Analysis with two-way Anova ** $p < 0.05$ *** $p < 0.001$ **** $p < 0.0001$. The graph shows the mean of three independent experiments*

The data obtained from the RTCA software program for the different treatment groups was used to plot the graph of time against the cell index.

As seen in Figure 4.2.4, 24 and 48 hours after CQ or CPT treatment of SKOV-3 ovarian cancer cells transfected with miRNA-155 miRNA inhibitor or its negative control in normoxic conditions, there were no significant differences in the proliferation levels of the control groups and the individual treatment groups. After 72 hours of further incubation of miRNA-155 miRNA inhibitor or its negative control transfected SKOV-3 cells treated with CPT, a statistically significant difference was observed in the cell index level of the untransfected SKOV-3 cells and the cells transfected with miRNA-155 miRNA mimic and 24 hours later incubated with CPT for 72 hours. This decrease was also observed between the control group and the group transfected with the negative control and treated with CPT. This suggests that CPT decreases the proliferation rate of cells transfected with both miRNA-155 miRNA inhibitor and its negative control as well as when treated with miRNA-155 miRNA mimic and its negative control transfected cells.

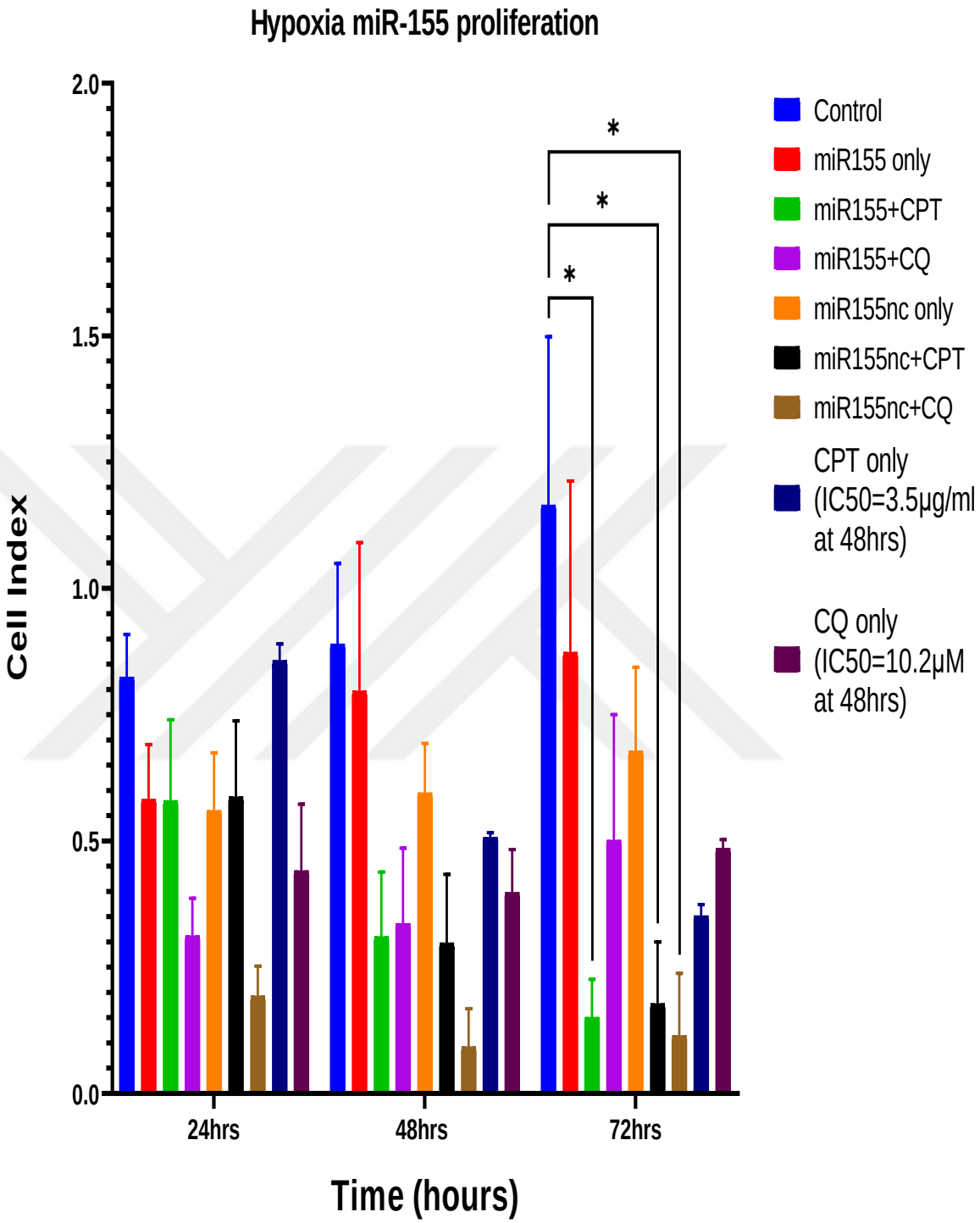

Figure 4.2.5. *Effect of Chloroquine and Camptothecin on the proliferation of SKOV-3 ovarian cancer cells transfected with miR-155 miRNA mimic and negative control in hypoxia. Cell index data are mean ± SEM of three independent experiments with n=6. Analysis with two-way Anova ** p < 0.05 *** p < 0.001 **** p < 0.0001. The graph shows the mean of three independent experiments*

The data obtained from the RTCA software program for the different treatment groups was used to plot the graph of time against the cell index.

As seen in Figure 4.2.5, 24 and 48 hours after CQ or CPT treatment of SKOV-3 ovarian cancer cells transfected with miRNA-155 miRNA mimic or its negative control in hypoxic conditions, there were no significant differences in the proliferation levels of the control groups and the individual treatment groups. After 72 hours of further incubation of miRNA-155 miRNA mimic or its negative control transfected SKOV-3 cells treated with CPT, a statistically significant difference was observed in the cell index level of the untransfected SKOV-3 cells and the cells transfected with miRNA-155 mimic and 24 hours later incubated with CPT for 72 hours. This decrease was also observed between the control group and the group transfected with the negative control and treated with CPT as well as the group transfected with the negative control and subsequently incubated with CQ. However, it is worthy of note that compared to the observed decrease under normoxia settings, the observed decrease had a higher cell index than as observed under similar treatment conditions in normoxia. This suggests that CPT decreases the proliferation rate of cells transfected with both the miRNA-155 mimic and its negative control under hypoxia but not as compared to the decrease obtained under normoxia settings.

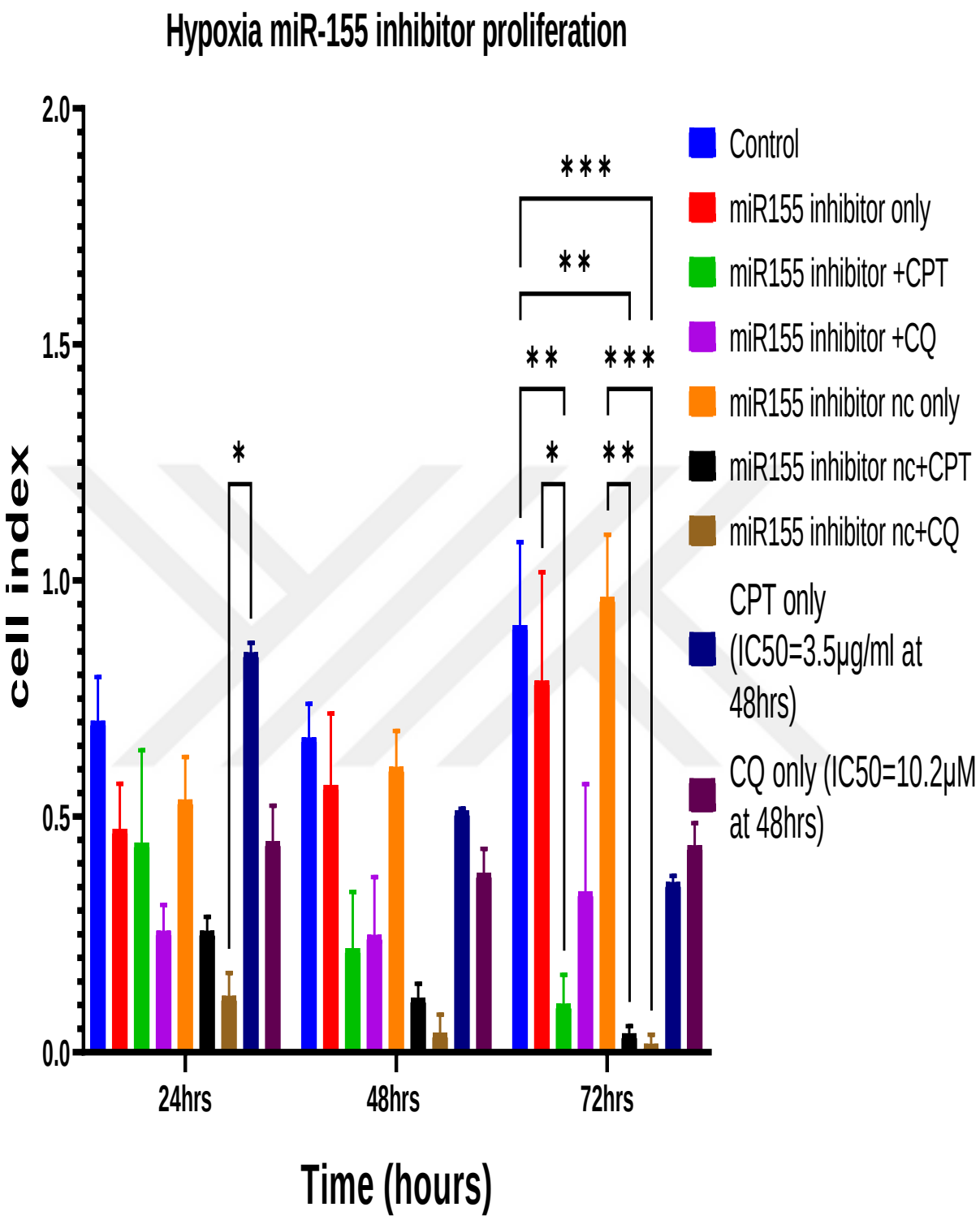

Figure 4.2.6. *Effect of Chloroquine and Camptothecin on the proliferation of SKOV-3 ovarian cancer cells transfected with miRNA-155 inhibitor and negative control in hypoxia. Cell index data are mean ± SEM of three independent experiments with n=6. Analysis with two-way Anova ** $p < 0.05$ *** $p < 0.001$ **** $p < 0.0001$. The graph shows the mean of three independent experiments*

The data obtained from the RTCA software program for the different treatment groups was used to plot the graph of time against the cell index.

As seen in Figure 4.2.6, apart from the statistically significant difference between the CPT -only treated group and the mimic negative control transfected group treated with CQ, 48 hours after CQ or CPT treatment of SKOV-3 ovarian cancer cells transfected with miRNA-155 inhibitor or its negative control in hypoxia conditions, there were no significant differences in the proliferation levels of the control groups and the individual treatment groups. After 72 hours of further incubation of miRNA-155 inhibitor or its negative control transfected SKOV-3 cells treated with CPT, a statistically significant difference was observed in the cell indexes of both the untransfected SKOV-3 cells, the miRNA-155 inhibitor only transfected group and the cells transfected with miRNA-155 inhibitor and 24 hours later treated with CPT for 72 hours. This decrease was also observed between the control group and the group transfected with the inhibitor-negative control and treated with CPT as well as the group transfected with the inhibitor-negative control and subsequently incubated with CQ.

A statistically significant decrease was also observed between the group transfected with inhibitor-negative control only and the group transfected with inhibitor-negative control and 24 hours later treated with CQ or CPT for 72 hours. However, it is worthy of note that compared to the observed decrease under normoxia settings, the observed decrease had a higher cell index than as observed under similar treatment conditions in normoxia. This suggests that CPT decreases the proliferation rate of cells transfected with both the miRNA-155 mimic and its negative control under hypoxia but not as compared to the decrease obtained under normoxia settings.

4.2.3. Effect of Chloroquine and Camptothecin on the migration of SKOV-3 ovarian cancer cells transfected with miRNA-155 mimic and miRNA-155 inhibitor in normoxia

SKOV-3 ovarian cancer cell line was seeded on CIM-plate and incubated in the RTCA system for 24 hours to ensure cell attachment in a normoxia incubator. At the end of the incubation period, cells were separately transfected with 100 nM miRNA-155 mimic, 100 nM miRNA-155 inhibitor, and 100 nM each of their negative controls. After 24 hours of transfection, the transfection media was removed and replaced with a medium containing either CQ (10.2 μM) or CPT (3.5 μg/ml), and the cells were left to incubate for 72 more hours. The CI values were measured in RTCA throughout the whole experiment. The analysis results of the experiment were normalized according to the time CQ or CPT was added in the RTCA software program and the CI values were determined. No transfection or inhibitor application was made

to the cells in the control group. Cell migration rates were calculated from the CI values obtained at the different time points, and compared to the control group. The results are given in two independent experiments with n=4 for the miRNA-155 mimic group and n=2. These are shown in figure 4.2.7 and figure 4.2.8

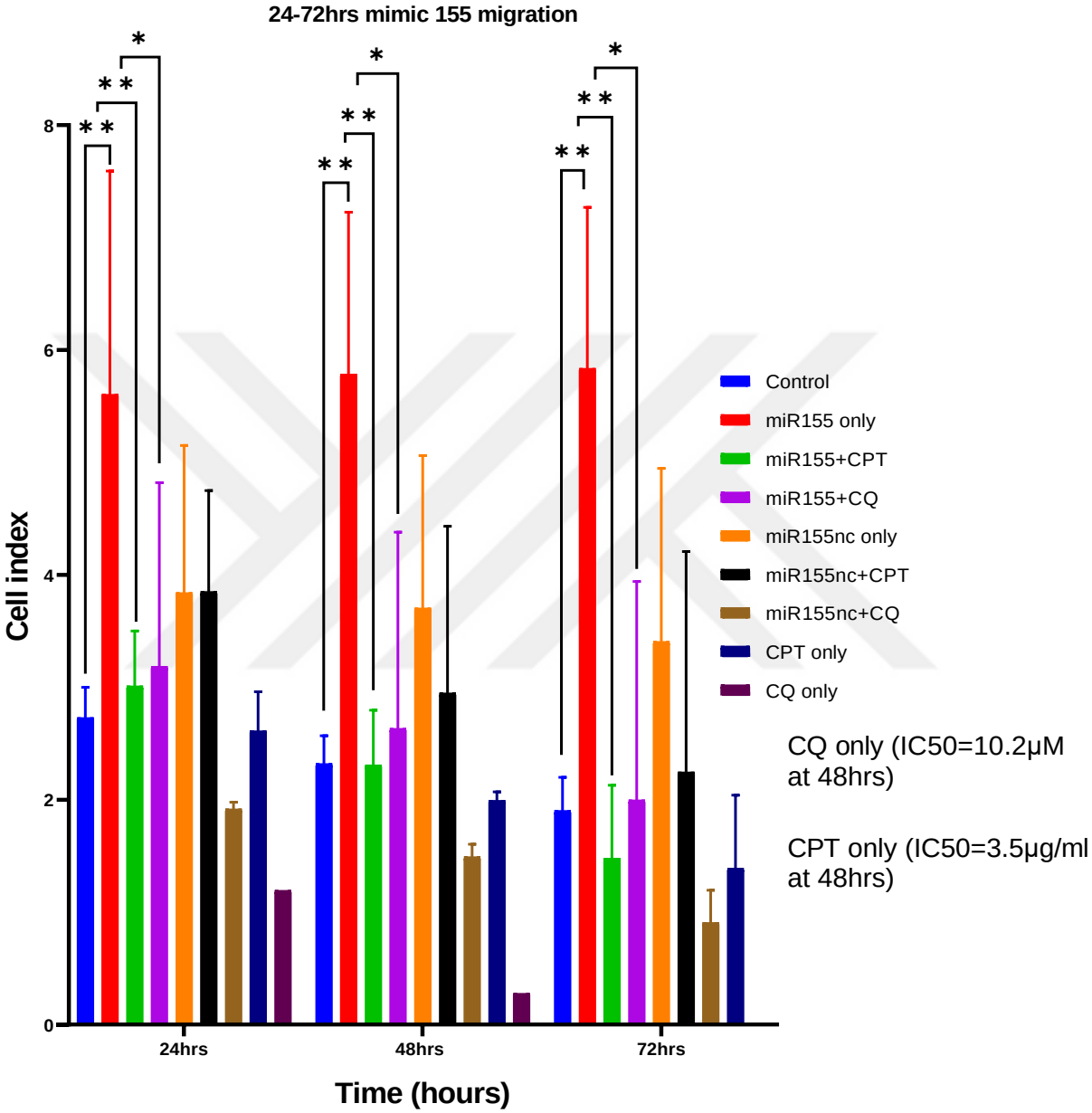

Figure 4.2.7. *Effect of Chloroquine and Camptothecin on the migration of SKOV-3 ovarian cancer cells transfected with miRNA-155 mimic and negative control in normoxia. Cell index data are mean ± SEM of three independent experiments with n=6. Analysis with two-way Anova ** p < 0.05 *** p < 0.001 **** p < 0.0001. The graph shows the mean of three independent experiments*

The data obtained from the RTCA software program for the different treatment groups was used to plot the graph of time against the cell index.

As seen in Figure 4.2.7, all through the selected time points (24, 48, and 72 hours) after CQ or CPT treatment of SKOV-3 ovarian cancer cells transfected with miRNA-155 mimic or its negative control in normoxic conditions, there was a significant increase in the migration rate of miRNA-155 mimic only transfected groups compared with the untransfected group, the two groups transfected with miRNA-155 mimic but later treated with either CQ or CPT.

This suggests that miRNA-155 mimic increases the migratory rate of SKOV-3 ovarian cancer cells *in vitro* regardless of the time difference of transfection. While the migration rate of every other treatment group decreased as time passed, groups treated only with miRNA-155 mimic showed the opposite effect. The addition of either CQ or CPT to the transfected cells rather decreased the migration rate of these cells.

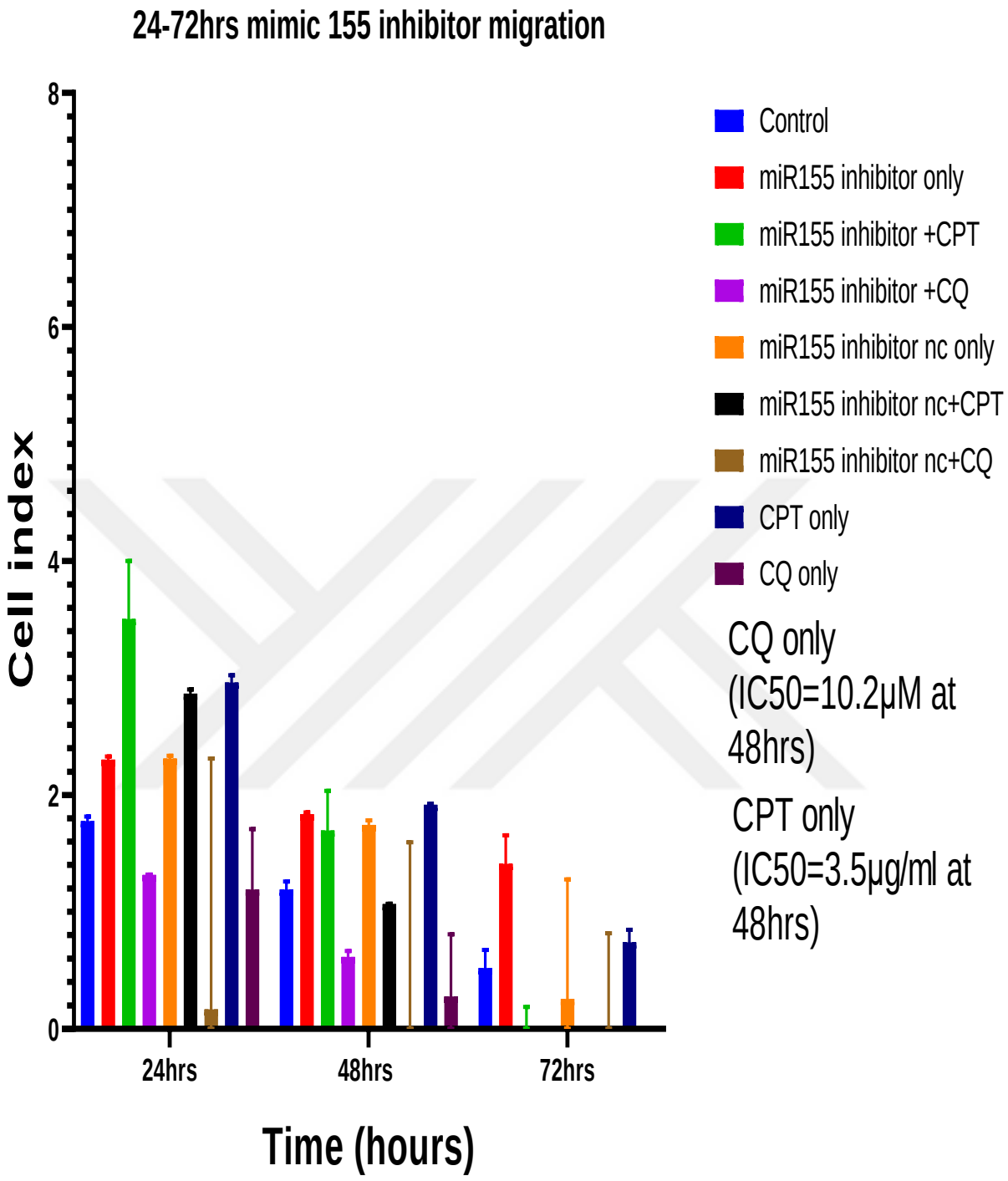

Figure 4.2.8. *Effect of Chloroquine and Camptothecin on the migration of SKOV-3 ovarian cancer cells transfected with miRNA-155 inhibitor and negative control in normoxia. Cell index data are mean ± SEM of three independent experiments with n=6. Analysis with two-way Anova ** $p < 0.05$ *** $p < 0.001$ **** $p < 0.0001$. The graph shows the mean of three independent experiments*

The data obtained from the RTCA software program for the different treatment groups was used to plot the graph of time against the cell index.

As seen in Figure 4.2.8, all through the selected time points (24, 48, and 72 hours) after CQ or CPT treatment of SKOV-3 ovarian cancer cells transfected with miRNA-155 inhibitor or its negative control in normoxic conditions, no significant differences in the migration rates were observed between all groups. However, there was a tendency for all the treatment groups to have a reduced migration rate as time passed and including the control group. It can be suggested that the miRNA-155 inhibitor inhibited the migration of SKOV-3 ovarian cancer cells as opposed to the observed effects of the miRNA-155 mimic. The migration rate decreased to negative values in some of the experimental cell groups other than the control cell group. The results obtained showed that although inhibition was observed in the migration rates of SKOV-3 cells, statistical analyzes showed that there was no significant difference between the variances of the experimental cell groups ($p > 0.05$). While the proliferation rates of SKOV-3 cells were not significantly affected in the miRNA-155 mimic-only treated groups, the migration of these cells transfected with this same mimic was significantly increased.

4.3. Autophagy Flux Results

4.3.1. Effect of Chloroquine and Camptothecin on the autophagy flux of SKOV-3 ovarian cancer cells transfected with miRNA-155 mimic and miRNA-155 inhibitor in normoxia or hypoxia condition

SKOV-3 ovarian cancer cell line was seeded in a 94-well plate and incubated for 24 hours to ensure cell attachment either in a normoxia or hypoxia incubator. At the end of the incubation period, cells were separately transfected with 100 nM miRNA-155 mimic, 100nM miRNA-155 inhibitor, and 100 nM each of their negative controls. After 24 hours of transfection, the transfection media was removed and replaced with a medium containing either CQ (10.2 μM) or CPT (3.5 μg/ml), and the cells were left to incubate for 48 more hours. At the end of the incubation, the cells were stained for autophagy flux with the Autophagosome detection reagent provided in the autophagy assay kit. After staining, the fluorescence intensity of each treatment group was measured under a fluorescence microscope (Leica, DMI 4000B, Germany) with a DAPI filter at 40× magnification. The autophagic vacuole is represented by the green particles in autophagic cells. Figure 4.3.1-4.3.4 show the **e**ffect of CQ and CPT on the autophagy of SKOV-3 ovarian cancer cells transfected with either miRNA-155 mimic, miRNA-155 inhibitor or their respective negative controls in normoxia or hypoxia.

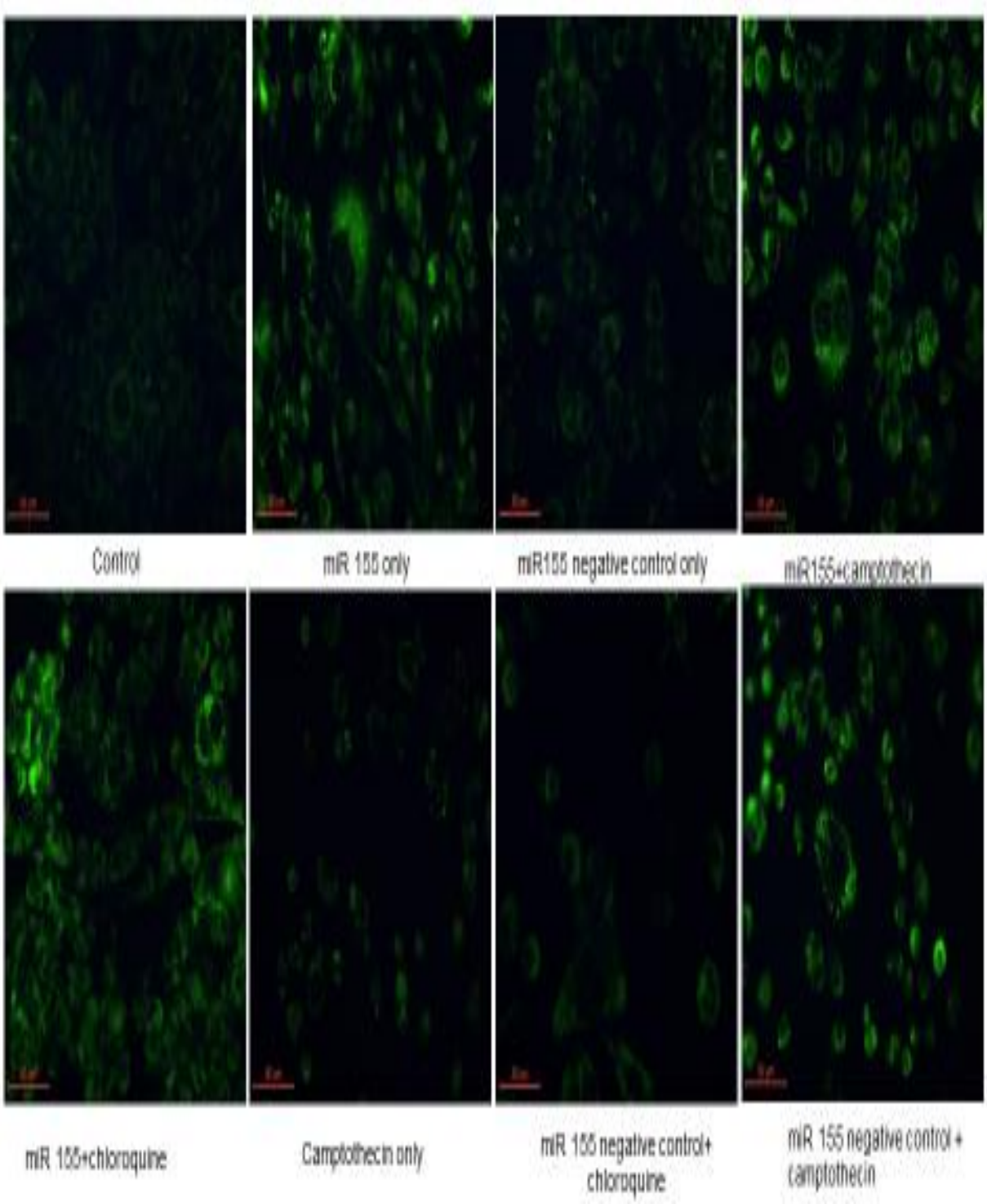

Figure 4.3.1. *Effect of Chloroquine and Camptothecin on the autophagy of SKOV-3 ovarian cancer cells transfected with miRNA-155 mimic and its negative control in normoxia. Cells were stained for autophagy flux with the Autophagosome detection reagent provided in the autophagy assay kit. After staining, the fluorescence intensity of each treatment group was measured under a fluorescence microscope (Leica, DMI 4000B, Germany) with a DAPI filter at 40× magnification.*

Table 4.3.1. *The average percentage of autophagosome vacuole in total cells transfected with miRNA-155 miRNA mimic and its negative control in normoxia and treated with either Chloroquine or Camptothecin*

Treatment Groups	**Average percentage of Autophagosome vacuole in total cells**
Control	30.70
miRNA-155 mimic	20.95
miR-155+CPT	51.31
miR-155NC+CPT	28.19
miR-155+ CQ	22.29
Negative Control (NC)	16.14
NC+CQ	57.74
CQ	41.81
CPT	24.62

As seen in Figure 4.3.1 and as represented in Table 4.3.1. The autophagy flux of SKOV-3 ovarian cancer cells was measured upon transfection with miRNA-155 mimic and its negative control in normoxia and upon treatment with either CQ or CPT. The percentage of cells expressing the autophagosome vacuole after staining with the autophagy assay kit was determined using the Imaje J software by setting a threshold for the autophagosome positive cells and contrasting these values with the total number of cells in each of the obtained images. The average value of four images are represented in Table 4.3.1. From the result, it can be seen that under normoxia the groups transfected with the miRNA-155 negative control and subsequently treated with CQ had the highest average percent of autophagosome vacuole with a value of 57.74%. The group transfected with the miRNA-155 negative control only had the least average percent of autophagosome vacuole with a value of 16.14%.

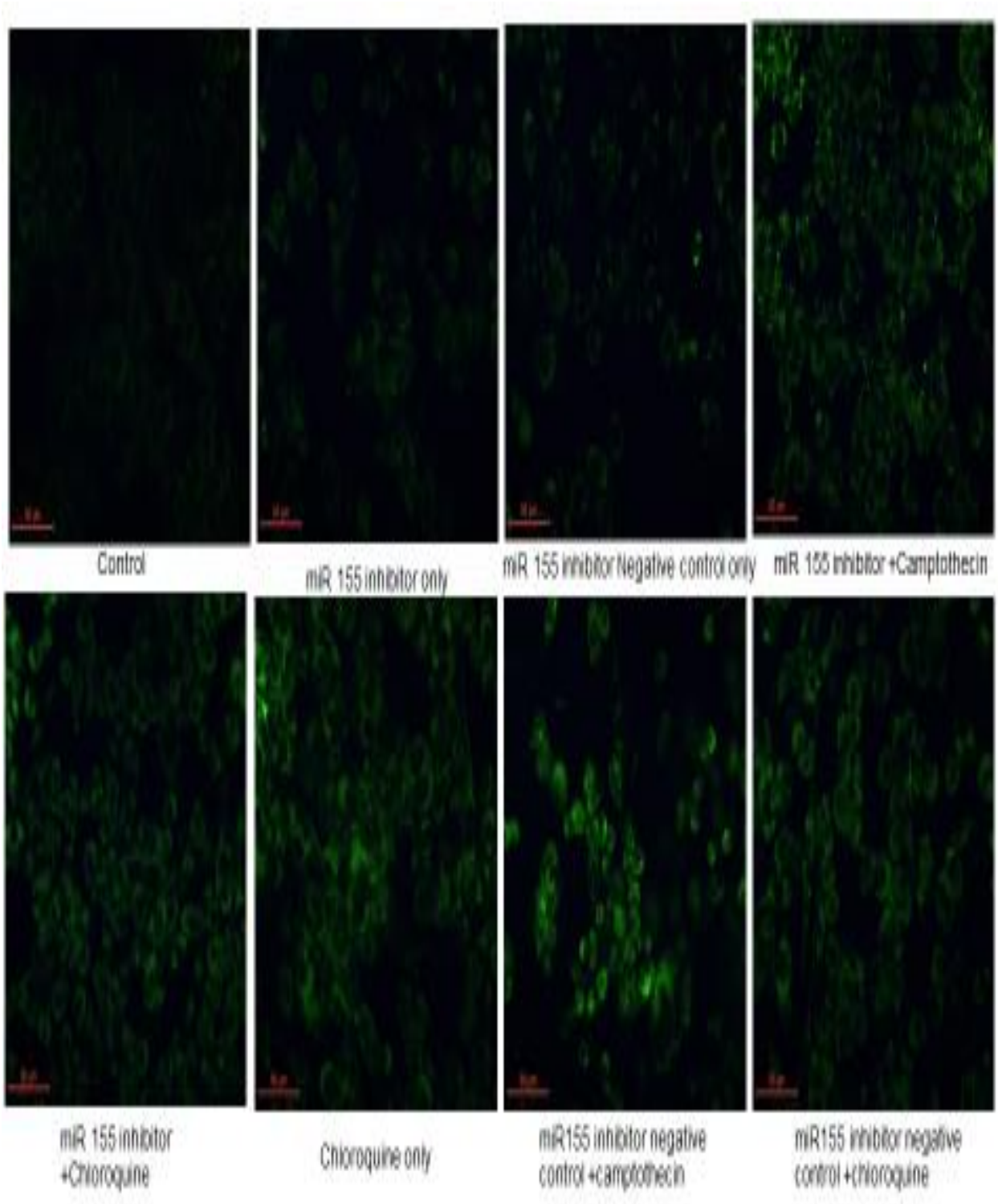

Figure 4.3.2. *Effect of Chloroquine and Camptothecin on the autophagy of SKOV-3 ovarian cancer cells transfected with miRNA-155 inhibitor and its negative control in normoxia. Cells were stained for autophagy flux with the Autophagosome detection reagent provided in the autophagy assay kit. After staining, the fluorescence intensity of each treatment group was measured under a fluorescence microscope (Leica, DMI 4000B, Germany) with a DAPI filter at 40X magnification*

Table 4.3.2. *The average percentage of autophagosome vacuole in total cells transfected with miRNA-155 inhibitor and its negative control in normoxia and treated with either Chloroquine or Camptothecin*

Treatment Groups	**Average percentage of Autophagosome vacuole in total cells**
Control	14.95
miRNA-155 inhibitor	21.60
miR-155 inhibitor+CPT	23.07
miR-155 inhibitor+CQ	29.52
miR-155 inhibitor NC+CPT	27.48
miR-155 inhibitor NC+CQ	30.04
miR-155 inhibitor NC	25.59
CPT	24.62
CQ	41.81

As seen in Figure 4.3.2 and as represented in Table 4.3.2, The autophagy flux of SKOV-3 ovarian cancer cells was measured upon transfection with miRNA-155 inhibitor and its negative control in normoxia and upon treatment with either CQ or CPT. The percentage of cells expressing the autophagosome vacuole after staining with the autophagy assay kit was determined using the Imaje J software by setting a threshold for the autophagosome positive cells and contrasting these values with the total number of cells in each of the obtained images. The average value of four images are represented in table 4.3.2. From the result, it is shown that under normoxia the groups treated with CQ only had the highest average percent of autophagosome vacuole with a value of 41.81% control untransfected and untreated group had the least average percent of autophagosome vacuole with a value of 14.95%.

This suggest that inhibiting miRNA-155 reduces autophagy flux in SKOV-3 ovarian cancer cells under normoxia.

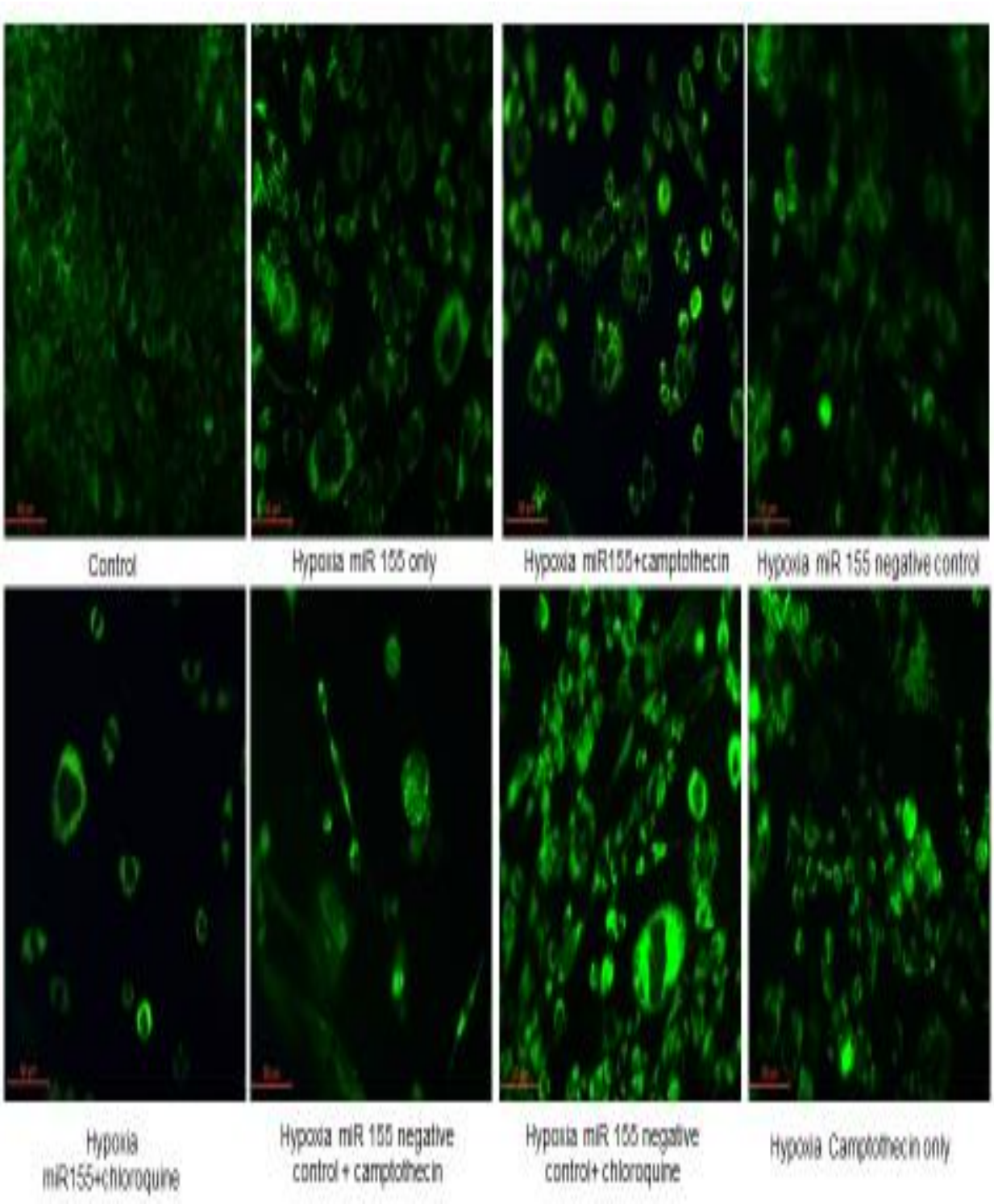

Figure 4.3.3. *Effect of Chloroquine and Camptothecin on the autophagy of SKOV-3 ovarian cancer cells transfected with miRNA-155 mimic and its negative control in hypoxia. Cells were stained for autophagy flux with the Autophagosome detection reagent provided in the autophagy assay kit. After staining, the fluorescence intensity of each treatment group was measured under a fluorescence microscope (Leica, DMI 4000B, Germany) with a DAPI filter at 40×magnification.*

Table 4.3.3. *The average percentage of Autophagosome vacuole in total cells transfected with miRNA-155 mimic and its negative control in hypoxia and treated with either Chloroquine or Camptothecin*

Treatment Groups	**Average percentage of Autophagosome vacuole in total cells**
Control	76.49
miRNA-155 mimic	21.63
miR-155 +CPT	48.91
miR-155 negative control (NC)	22.84
miR-155 negative control + CQ	65.07
miR-155 +CPT	53.96
miR-155 +CQ	57.81
CQ	30.04
CPT	91.75

As seen in Figure 4.3.3 and as represented in Table 4.3.3, The autophagy flux of SKOV-3 ovarian cancer cells was measured upon transfection with miRNA-155 mimic and its negative control in hypoxia and upon treatment with either CQ or CPT. The percentage of cells expressing the autophagosome vacuole after staining with the autophagy assay kit was determined using the Imaje J software by setting a threshold for the autophagosome positive cells and contrasting these values with the total number of cells in each of the obtained images. The average value of four images are represented in table 4.3.3. From the result, we can see that under hypoxia the groups treated with CPT only had the highest average percent of autophagosome vacuole with a value of 91.75%. The group transfected with the miRNA-155 only had the least average percent of autophagosome vacuole with a value of 21.63%.

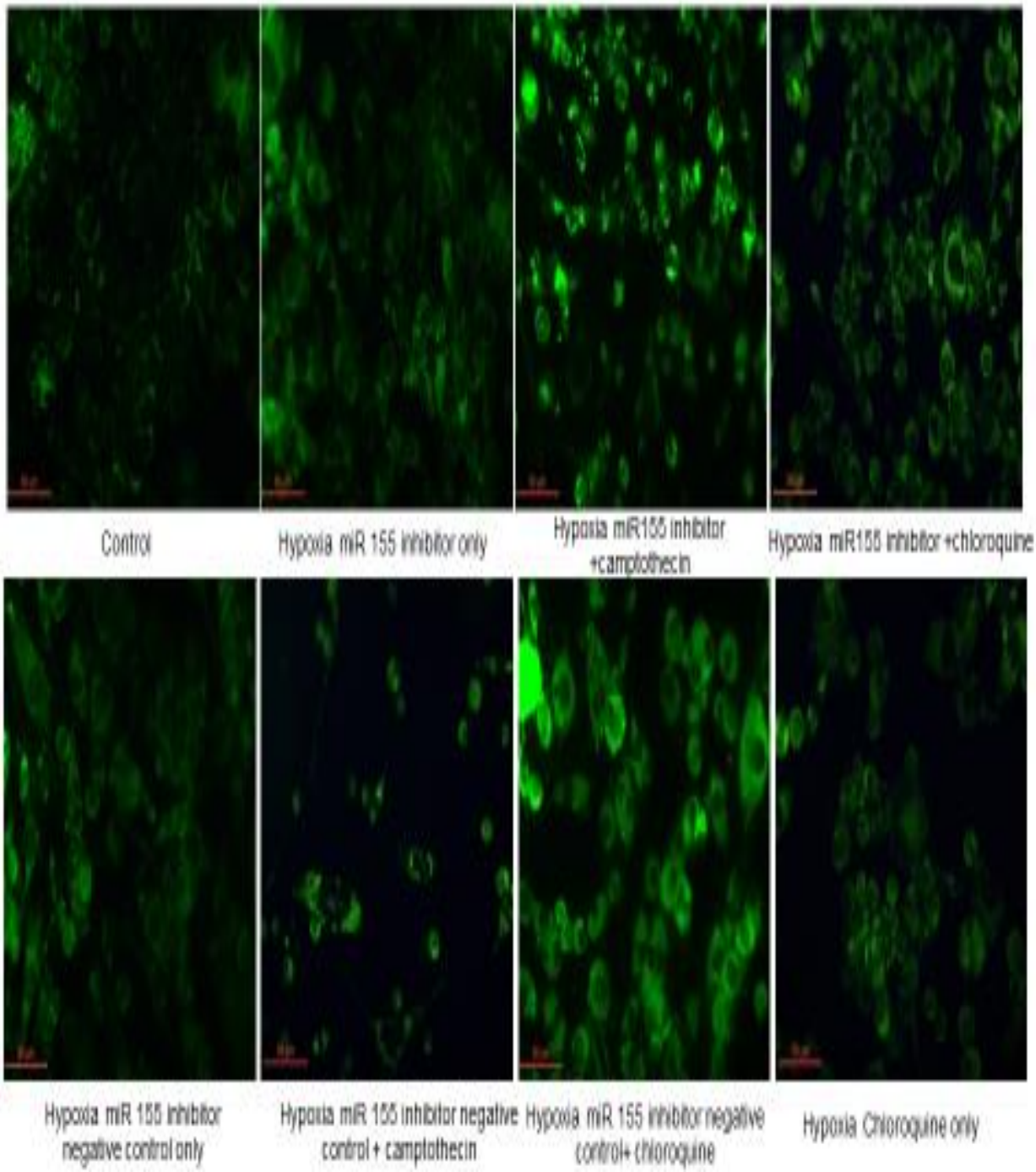

Figure 4.3.4. *Effect of Chloroquine and Camptothecin on the autophagy of SKOV-3 ovarian cancer cells transfected with miRNA-155 inhibitor and its negative control in hypoxia. Cells were stained for autophagy flux with the Autophagosome detection reagent provided in the autophagy assay kit. After staining, the fluorescence intensity of each treatment group was measured under a fluorescence microscope (Leica, DMI 4000B, Germany) with a DAPI filter at 40× magnification.*

Table 4.3.4. *The average percentage of Autophagosome vacuole in total cells transfected with miRNA-155 inhibitor and its negative control in hypoxia and treated with either Chloroquine or Camptothecin*

Treatment Groups	**Average percentage of Autophagosome vacuole in total cells**
Control	23.04
miRNA-155 inhibitor	40.78
miR-155 inhibitor (NC)	11.97
miR-155 inhibitor (NC) + CPT	76.61
miR-155 inhibitor+CPT	39.23
miR-155 inhibitor +CPT	37.76
miR-155 inhibitor +CQ	36.09
CPT	91.75
CQ	30.04

As seen in Figure 4.3.4 and as represented in Table 4.3.4, The autophagy flux of SKOV-3 ovarian cancer cells was measured upon transfection with miRNA-155 inhibitor and its negative control in hypoxia and upon treatment with either CQ or CPT. The percentage of cells expressing the autophagosome vacuole after staining with the autophagy assay kit was determined using the Imaje J software by setting a threshold for the autophagosome positive cells and contrasting these values with the total number of cells in each of the obtained images. The average value of four images are represented in table 4.3.4. From the result, it is shown that under hypoxia the groups treated with CPT only had the highest average percent of autophagosome vacuole with a value of 91.75%. control untransfected and untreated group had the least average percent of autophagosome vacuole with a value of 23.04%.

This suggest that inhibiting miRNA-155 reduces autophagy flux in SKOV-3 ovarian cancer cells under normoxia.

4.3.2. Effect of Chloroquine and Camptothecin on the morphology of SKOV-3 ovarian cancer cells transfected with miRNA-155 miRNA mimic and miRNA-155 miRNA inhibitor in normoxia

SKOV-3 ovarian cancer cell line was seeded in a 94-well plate and incubated for 24 hours to ensure cell attachment in a normoxia incubator. At the end of the incubation period, cells were separately transfected with 100 nM miRNA-155 mimic, 100 nM miRNA-155 inhibitor, and 100nM each of their negative controls. After 24 hours of transfection, the transfection media was removed and replaced with a medium containing either CQ (10.2 μM) or CPT (3.5

μg/ml), and the cells were left to incubate for 48 more hours. At the end of the incubation, the cells were stained for autophagy flux with the Autophagosome detection reagent provided in the autophagy assay kit. After staining, the morphology of each treatment group was measured under a light microscope (Leica, DMI 4000B, Germany) at 40× magnification. Figure 4.3.5 and 4.3.6 show the **e**ffect of CQ and CPT on the morphology of SKOV-3 ovarian cancer cells transfected with either miRNA-155 mimic, miRNA-155 inhibitor or their respective negative controls under normoxia.

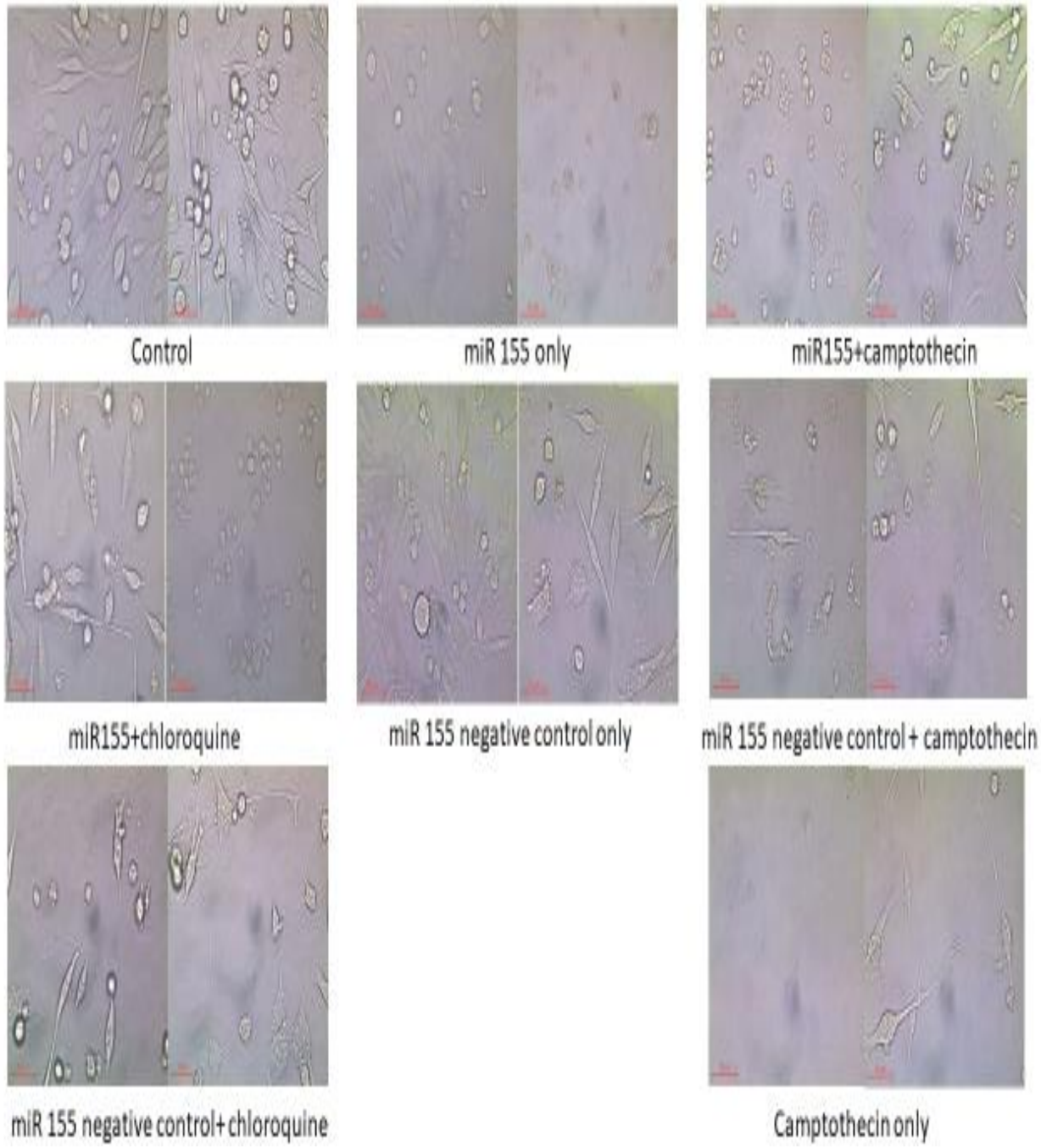

Figure 4.3.5. *Effect of Chloroquine and Camptothecin on the morphology of SKOV-3 ovarian cancer cells transfected with miRNA-155 mimic and its negative control in normoxia. Cells were stained for autophagy flux with the Autophagosome detection reagent provided in the autophagy assay kit. After staining, the morphology of each treatment group was measured under a light microscope (Leica, DMI 4000B, Germany) at 40× magnification.*

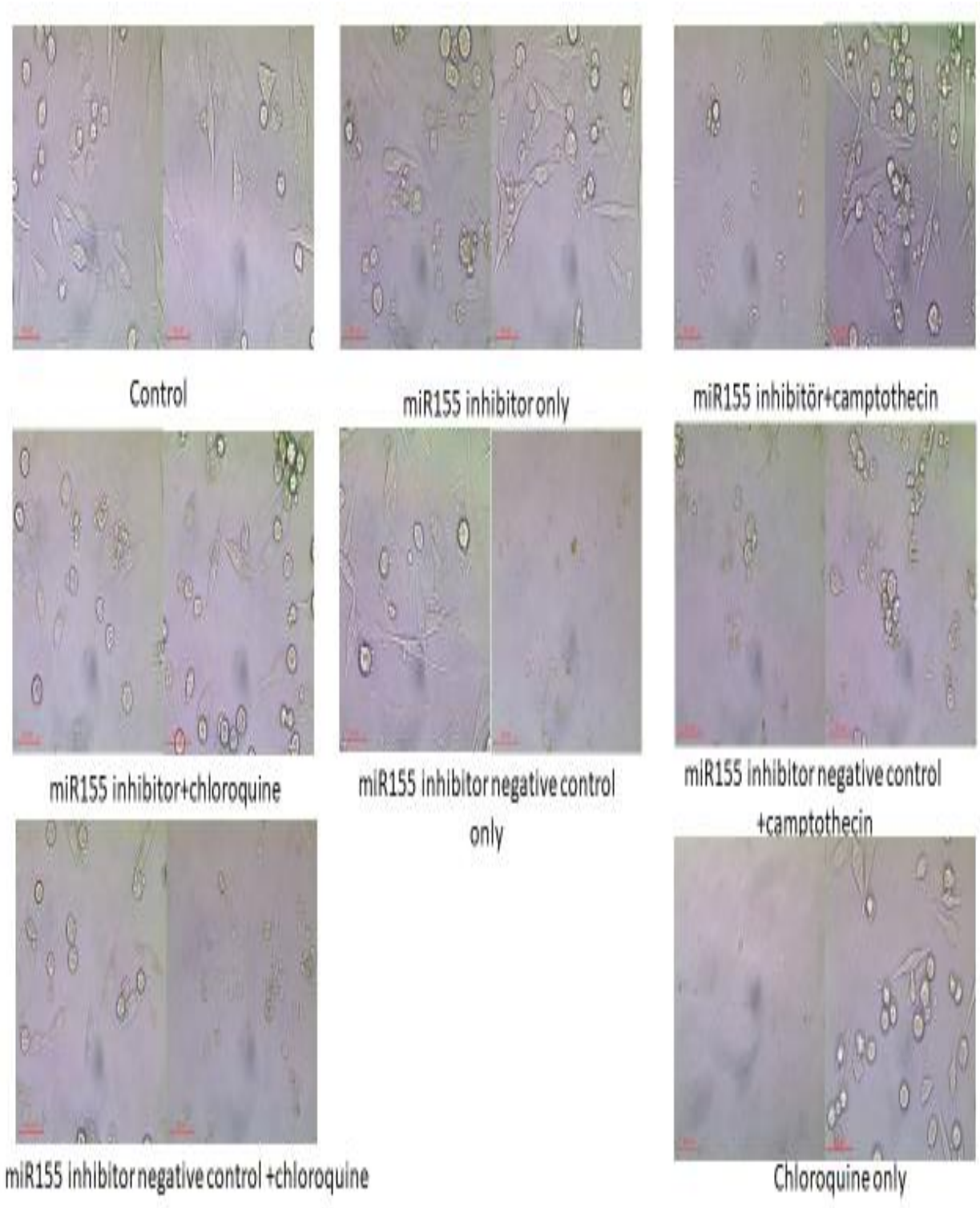

Figure 4.3.6 *Effect of Chloroquine and Camptothecin on the morphology of SKOV-3 ovarian cancer cells transfected with miRNA-155 inhibitor and its negative control in normoxia. Cells were stained for autophagy flux with the Autophagosome detection reagent provided in the autophagy assay kit. After staining, the morphology of each treatment group was measured under a light microscope (Leica, DMI 4000B, Germany) at 40× magnification.*

As seen in Figure 4.3.5 and 4.3.6 the morphologhy of SKOV-3 ovarian cancer cells was checked upon transfection with either miRNA-155 mimic or miRNA-155 inhibitor and their negative control in normoxia and treatment with either CQ or CPT. From the images taken, we could see that the while the cells looked quite okay in both the control groups and the group transfected with mir-155 inhibitor, the group transfected with the miR-155 looked differently. It seems as though the cells transfected with the miRNA-155 mimic died more as a result of the transfection than is observed for the miRNA-155 inhibitor. The morphology looked much better the miRNA-155 mimic transfected cells were treated with either CPT or CQ. This suggests that these compounds helped to preserve the morphology of these cells.

5. DISCUSSION, CONCLUSIONS AND RECOMMENDATIONS

A lot of people die from cancer every year throughout the world. The field of anticancer drug development has experienced rapid and substantial advancement in the past few decades. In spite of the developments, cancer still holds the second position in the ranking of major causes of death after cardiovascular disease (Swamy et al., 2021).Women worldwide easily develop ovarian cancer. On the list of the most commonly diagnosed cancers in women world-wide, ovarian cancer ranks eighth. Despite the availability of novel treatment options, about one-half of ovarian cancer patients still die within five years of diagnosis. Therefore more potent and novel agents for treating ovarian cancer still have to be developed (X. Wang et al., 2021).

The field of cancer diagnosis and therapy is recently exploring the microRNA biology route. MicroRNA are small 19-25 nucleotide-long endogenous non-coding RNAs that possess the ability to regulate the expression of genes in humans and a lot of other organisms. MiRNA has been reported to be involved in several biological processes such as proliferation, autoph-agy, as well as ovarian cancer initiation, progression, and resistance to therapy. They have also been implicated in various biological response of cells to oxygen deficiency-hypoxia. They function as important regulators in very many physiological phenomenon such as cellular me-tabolism, signaling pathways regulation, embryonic development, tissue differentiation etc. (Zou et al., 2021) MiR-210 is a putative hypoxia-induced miRNA. It has been reported to inhibit EOC apoptosis in-vitro while increasing their proliferation and migration rates. It is interesting to note that when miR-210 is deleted, ovarian cancer still progresses and the cell cycle is dysregulated and thereby depicting a context-specific role of miRNAs (Pereira et al., 2021). MiRNA-155 has been studied across different cellular contexts and research aims. Nu-merous data has been published on the impact of this specific miRNA on various pathological, physiological and developmental conditions. Chen et al was able to study the involvement of miR-155 in chemotherapy resistance in osteosarcoma therapy (Chen et al., 2014). Sul et al., investigated the role of miR-155 under inflammatory conditions as it connects with bone loss (Sul et al., 2018). The tumor promoting and suppressing function of this miRNA has also been studied across several cancer types such as melanoma, gastric cancer, oral squamous cell car-cinoma, nasopharyngeal carcinoma etc. (Chen et al., 2016). MiRNA-155 is therefore best de-scribed as a multifunctional miRNA whose function must be investigated several different physiological and pathological conditions as well as treatment groups including ovarian cancer

(Zhang et al., 2017; Zou et al., 2021; Xia & Zhao, 2019). The impact of these multifunctional miRNAs on autophagy in SKOV-3 ovarian cancer cells has not been fully elucidated.

In this thesis, the proliferative, migration, and autophagic impact of transfecting SKOV-3 ovarian cancer cells with either miRNA-155 mimic, miRNA-155 inhibitor, or their respective negative controls in the presence of either CQ or CPT together with incubation under hypoxia or normoxia conditions were investigated.

In the MTT assay, the cytotoxic effect of CQ, which is an autophagy inhibitor, and CPT, which is an autophagy inducer on SKOV-3 ovarian cancer cells were tested. The IC_{50} values were determined. We observed a significant decrease in the cell viability of SKOV-3 ovarian cancer cells treated with increased concentrations of either CQ or CPT. The IC_{50} value of CPT (3.5 μg/ml) determined at 48 hours of incubation with SKOV-3 ovarian cancer cells in our study is in line with the findings of Shen et al who reported an IC_{50} value of 3.09 μg/ml for SKOV-3 ovarian cancer cells incubated with CPT for 48 hours (Shen et al., 2009). On the other hand, we reported an IC_{50} value of 10 μM for CQ after 48 hours of incubation with SKOV-3 cells. Even though not many studies has reported the IC_{50} value of CQ in SKOV-3 ovarian cancer cells at 48 hours of incubation, this value contradicts those observed by Ovejero-Sánchez et al who reported an IC_{50} value of 22.28 μM at 72 hours of incubation with SKOV-3 cancer cells (Ovejero-Sánchez et al., 2021). However, the value parallels the concentration used by El-Mais et al., who employed 10 μM for their autophagy assay in SKOV-3 ovarian cancer cells (El-Mais et al., 2021). The discrepancy in the IC_{50} value obtained in our study and other studies may be a result of the different CQ compound used. However, the reported IC_{50} value fits closely with CQ therapeutic dose administered routinely at 250 mg daily. The IC_{50} value obtained in SKOV-3 ovarian cancer cells is much lower than those obtained for other cancer cell types and this may highlight the fact that SKOV-3 ovarian cancer cells have a higher level of sensitivity to CQ than other cancers (Fukuda et al., 2015).

The expression levels of miRNA-155 was over and under expressed in SKOV-3 ovarian cancer cells by transfecting the cells with either miRNA-155 mimic or miRNA-155 inhibitor. Furthermore, cell migration rates, cell proliferation and autophagy flux of SKOV-3 ovarian cancer cells were determined by establishing cell group models with or without the presence or absence of either CQ or CPT under normoxic or hypoxic conditions.

Our finding that the transfection of SKOV-3 ovarian cancer cells with miRNA-155 mimic alone did not produce a significant change in the proliferation levels of SKOV-3 ovarian cancer cells under normoxic and hypoxic conditions is in agreement with the findings of Ysrafil

et al., who reported that miRNA-155-5p does not diminish the viability of ovarian cancer cells *in vitro* alone. It only diminished the viability of these cells when it is conjugated with carriers such as chitosan nanoparticles by targeting HIF-1α (Ysrafil et al., 2020). It is also important to note that while the cells transfected with miRNA-155 mimic under normoxic conditions showed a tendency to increase proliferation, under hypoxia, a tendency for a reduction in proliferation was observed. This may be as a result of the stress experienced by the SKOV-3 cells under hypoxia treatment. In addition, compared with the results obtained for the transfection with miRNA-155 mimic, the proliferation of SKOV-3 showed a tendency to be reduced when transfected with miRNA-155 inhibitor alone, under both hypoxic and normoxic conditions. However, other studies show some anti-proliferative properties of miRNA-155 such as the findings of Qin et al., who reported a suppressive function of miRNA-155 in ovarian cancer initiating cells (Qin et al., 2013). Wan et al., also reported the attenuation effect of miRNA-155 on the proliferation of CNE and HeLa cells (Wan et al., 2014). It, therefore, suggests that this miRNA behaves differently depending on the type of cells and the cellular context.

Our finding that miRNA-155 drastically reduces the proliferation of SKOV-3 ovarian cells when combined with drug compounds such as CQ or CPT is much expected and is in line with the study of Chen et al., who combined miRNA-155 transfection with cisplatin treatment which led to a reduction in the IC_{50} value of SKOV-3 ovarian cancer cells as compared to when these cells are treated with cisplatin alone (W. Chen et al., 2016). However, it is in disagreement with the findings of Chen et al., who reported that miRNA-155 overexpression in Saos-2 osteosarcoma cells helped to ameliorate the cell proliferation decrease caused by anticancer drugs (Chen et al., 2014). These findings are suggestive of the tumor-suppressive and tumor-promoting potentials of the combinatory use of miRNA-155 with anticancer drugs. In vivo studies to validate these claims are therefore recommended.

The results obtained from the RTCA device for the migration rate of SKOV-3 ovarian cancer cells transfected with either miRNA-155 mimic miRNA-155 inhibitor show that miR-155 miRNA mimic drastically increased the migration rates of SKOV-3 ovarian cancer cells *in vitro* by more than two folds. This observation closely aligns with the findings of Xia and Zhao, who observed that miRNA-155 promoted migration and invasion of KGN cells (Xia and Zhao, 2019). Furthermore, although treatment of these transfected cells with either CPT or CQ significantly reduced the migration rates of the cells in this group when compared with the miRNA-155 only transfected group, the decrease was not as much as that observed for the untransfected groups treated with only CPT or CQ which are the groups treated with these

compounds alone. In addition, transfection of SKOV-3 ovarian cancer cells with miRNA-155 miRNA inhibitor showed a tendency to decrease the migration rates of these cells *in vitro*. This decrease was also observed for the groups transfected with miRNA-155 miRNA inhibitor and subsequently treated with either CPT or CQ. This further validates the potential of miRNA-155 miRNA mimic to increase the migration of SKOV-3 ovarian cancer *in vitro* upon migration.

Autophagosomes are formed in autophagy after degraded substances called cargo have been encapsulated. These cargo are then taken to the lysosome after which the lysosome fuses with the autophagosome to form an autolysosome. Once there is a disruption in the fusion of these two, then the accumulation of autophagosome in the cell may occur (Zhang et al., 2020). The effect of transfecting SKOV-3 cells with miRNA-155 mimic or its inhibitor on autophagy flux as well as the morphological changes was measured. Treatment of CPT was employed as a positive control to induce autophagy while treatment of CQ was employed as a negative control to inhibit autophagy. Our study showed that under normoxia, miRNA-155 mimic largely decreased the autophagy flux of SKOV-3 ovarian cancer cells when compared to the control, un-transfected and untreated group. The miRNA-155 miRNA inhibitor, when transfected alone increased the autophagy flux of SKOV-3 ovarian cancer cells when compared to the control, untransfected and untreated group as well as the miRNA-155 transfected group.
Under hypoxic conditions, we observed that the miRNA-155 mimic also greatly reduced the autophagy flux when compared with the control un-transfected, untreated group. It reduced the percent of SKOV-3 ovarian cancer cells with autophagosome vacuoles of when combined with CPT as compared with the groups treated with CPT only. It is worthy of note that under hypoxia, the control group had a high level of autophagy flux. This is particularly interesting because hypoxia is known to be an inducer of autophagy. On the other hand, under hypoxia, the miRNA-155 inhibitor showed an opposite effect when compared with the results obtained for the percent autophagosome vacuole of the miRNA-155 mimic. It lead to a more than 100% increase in the autophagy flux of SKOV-3 ovarian cancer cells when compared with the control and the miRNA-155 transfected group. These findings are in line with the observed morphological changes of these treatment groups. Particularly under normoxia, we could see that while the cells looked quite okay in both the control groups and the group transfected with the miRNA-155 inhibitor, SKOV-3 ovarian cancer cells shrinked more upon transfection with the miRNA-155 than is observed for the miRNA-155 inhibitor transfected groups and the control group. The morphology looked much better when the miRNA-155 mimic transfected cells were

treated with either CPT or CQ. This suggests that these compounds helped to preserve the morphology of these cells and that miRNA-155 induced an autophagy cell death while its repression supported a protective autophagy under both hypoxic and normoxic conditions.

Although numerous studies has reported the role of miRNA-155 on autophagy in several cell contexts, to the best of our knowledge, no report has been given on its impact on the autophagy of SKOV-3 ovarian cancer cells. For example, Wang et al reported that miRNA-155 promotes autophagy in cervical cancer through the MTOR pathway (Wang et al., 2018) .Wan et al, also reported that miRNA-155 upon induction by hypoxia induces autophagy (Wan et al., 2014). Chen et al., reported that miRNA-155 induces autophagy in osteosarcoma cells thereby facilitating resistance to drug treatment (Chen et al., 2014). Sul et al., also reported that miRNA-155 is an inducer of autophagy in osteoclasts (Sul et al., 2018). To the best of our knowledge, our study is one of the first to elucidate the role of miRNA-155 on the autophagy of SKOV-3 ovarian cancer cells. We propose that based on the obtained autophagy flux and morphological results, the overexpression of miRNA-155 induces autophagy cell death in SKOV-3 ovarian cancer cells while its repression supported a protective autophagy form under both hypoxic and normoxic conditions.

The overexpression of miRNA-155 expression may be a good strategy to use for the inhibition of ovarian cancer cell differentiation by inhibiting protective autophagy, especially in combination with other therapeutic options. In conclusion, we demonstrate that miRNA-155 is very crucial for maintaining the proliferation, migration and autophagy of ovarian cancer cells. It is required to promote the proliferation and migration of SKOV-3 ovarian cancer cells. It decreases the autophagy flux in these cells and therefore serves as an autophagic cell death inducer. Combination with either CQ or CPT further affects these signatures. The present study has further elucidated on the role of miRNA-155 miRNA on many signatures of SKOV-3 ovarian cancer cells, particularly on autophagy. These overall results validate the fact that miRNA-155 is an important player in the anticancer drug-induced autophagy in numerous cancer cells including SKOV-3 ovarian cancer cells. These findings may be employed for use as a route to explore for the development of diagnosis and treatment options for ovarian cancer patients. However, *in vivo* experiments are highly recommended to further elucidate on these findings and their mechanism of actions.

REFERENCES

Akkoc, Y., and Gozuacik, D. (2020). MicroRNAs as major regulators of the autophagy pathway. *Biochimica et Biophysica Acta (BBA) - Molecular Cell Research*, *1867*(5), 118662.

Ashrafizadeh, M., Zarrabi, A., Orouei, S., Kiavash H., Hakimi, A., Amirhossein Z., Daneshi, S., Samarghandian, S., Baradaran, B., and Najafi, M. (2021). MicroRNA-mediated autophagy regulation in cancer therapy: The role in chemoresistance/chemosensitivity. *European Journal of Pharmacology*, *892*, 173660.

Barnes, B.M., Nelson, L., Tighe, A., Morgan, R.D., McGrail, J., and Taylor, S.S. (2020). Classification of ovarian cancer cell lines using transcriptional profiles defines the five major pathological subtypes. *BioRxiv*, 2020.07.14.202457.

Boulefour, W., Rowinski, E., Louati, S., Sotton, S., Wozny, A. S., Moreno-Acosta, P., Mery, B., Rodriguez-Lafrasse, C., and Magne, N. (2021). A Review of the Role of Hypoxia in Radioresistance in Cancer Therapy. *Medical Science Monitor*, *27*, e934116-1–e934116-7.

Carey, P., Low, E., Harper, E., and Stack, M.S. (2021). Metalloproteinases in Ovarian Cancer. *International Journal of Molecular Sciences*, *22*(7).

Catani, M.V., Gasperi, V., Savini, I., Zingale, V.D., Gugliandolo, A., and Mazzon, E. (2021). MiR-155: An Important Regulator of Neuroinflammation. *International Journal of Molecular Sciences*, *23*(1), 90.

Chen, L., Jiang, K., Jiang, H., and Wei, P. (2014). miR-155 mediates drug resistance in osteosarcoma cells via inducing autophagy. *Experimental and Therapeutic Medicine*, *8*(2), 527–532.

Chen, W., Huang, L., Hao, C., Zeng, W., Luo, X., Li, X., Zhou, L., Jiang, S., Chen, Z., and He, Y. (2016). MicroRNA-155 promotes apoptosis in SKOV3, A2780, and primary cultured ovarian cancer cells. *Tumor Biology*, *37*, 9289–9299.

Chen, Y., and Gibson, S.B. (2021). Three dimensions of autophagy in regulating tumor growth: cell survival/death, cell proliferation, and tumor dormancy. *Biochimica et Biophysica Acta (BBA) - Molecular Basis of Disease*, *1867*(12), 166265.

Chmurska, A., Matczak, K., and Marczak, A. (2021). Two Faces of Autophagy in the Struggle against Cancer. *International Journal of Molecular Sciences*, *22*(6), 1–29.

Diori Karidio, I., and Sanlier, S.H. (2021). Reviewing cancer's biology: an eclectic approach. *Journal of the Egyptian National Cancer Institute 2021 33:1*, *33*(1), 1–17.

Provencher, D.M., Lounis, H., Champoux L., Tétrault M., Manderson E.N., Wang J.C., Eydoux P., Savoie R., Tonin P.N., Mes-Masson A.M. (2000) Characterization of four novel epithelial ovarian cancer cell lines. *In Vitro Cell Dev Biol Anim.* Jun; 36(6):357-61.

El-Mais, N., Fakhoury, I., Abdellatef, S., Abi-Habib, R., and El-Sibai, M. (2021). Human recombinant arginase I [HuArgI (Co)-PEG5000]-induced arginine depletion inhibits ovarian cancer cell adhesion and migration through autophagy-mediated inhibition of RhoA. *Journal of Ovarian Research*, *14*(1).

Falzone, L., Scandurra, G., Lombardo, V., Gattuso, G., Lavoro, A., Distefano, A. B., Scibilia, G., and Scollo, P. (2021). A multidisciplinary approach remains the best strategy to improve and strengthen the management of ovarian cancer (Review). *International Journal of Oncology*, *59*(1).

Fukuda, T., Oda, K., Wada-Hiraike, O., Sone, K., Inaba, K., Ikeda, Y., Miyasaka, A., Kashiyama, T., Tanikawa, M., Arimoto, T., Kuramoto, H., Yano, T., Kawana, K., Osuga, Y., and Fujii, T. (2015). The anti-malarial chloroquine suppresses proliferation and overcomes cisplatin resistance of endometrial cancer cells via autophagy inhibition. *Gynecologic Oncology*, *137*(3), 538–545.

Gaitskell, K., Hermon, C., Barnes, I., Pirie, K., Floud, S., Green, J., Beral, V., and Reeves, G. K. (2022). Ovarian cancer survival by stage, histotype, and pre-diagnostic lifestyle factors, in the prospective UK Million Women Study. *Cancer Epidemiology*, *76*, 102074.

Guan, Y., Wang, G., Fails, D., Nagarajan, P., and Ge, Y. (2020). Unraveling cancer lineage drivers in squamous cell carcinomas. *Pharmacology & Therapeutics*, *206*, 107448.

Ha, H. I., Cho, S. H., Lim, J., Lee, Y. J., Yoo, C. W., Won, Y. J., and Lim, M. C. (2021). Incidence and treatment outcomes of ovarian sarcoma compared to epithelial ovarian cancer from the national cancer registry. *Gynecologic Oncology*, *163*(3), 506–510.

Hallas-Potts, A., Dawson, J.C., and Herrington, C.S. (2019). Ovarian cancer cell lines derived from non-serous carcinomas migrate and invade more aggressively than those derived from high-grade serous carcinomas. *Scientific Reports 2019 9:1*, *9*(1), 1–10.

Heng, Y., Liang, Y., Zhang, J., Li, L., Zhang, W., Jiang, Y., Wang, S., and Jia, L. (2021). Camptothecin Inhibits Neddylation to Activate the Protective Autophagy Through NF-κB/AMPK/mTOR/ULK1 Axis in Human Esophageal Cancer Cells. *Frontiers in Oncology*, *11*.

Huang, L., Liu, J., Bie, C., Liu, H., Ji, Y., Chen, D., Zhu, M., and Kuang, W. (2022). Advances in cell death - related signaling pathways in acute-on-chronic liver failure. *Clinics and Research in Hepatology and Gastroenterology*, *46*(2), 101783.

Hyttinen, J.M.T., Blasiak, J., Felszeghy, S., and Kaarniranta, K. (2021). MicroRNAs in the regulation of autophagy and their possible use in age-related macular degeneration therapy. *Ageing Research Reviews*, *67*, 101260.

Ibragimova, M.K., Kokorina, E. v., Tsyganov, M.M., Churuksaeva, O.N., and Litviakov, N. v. (2021). Human papillomavirus and ovarian cancer (review of literature and meta-analysis). *Infection, Genetics and Evolution*, *95*, 105086.

Ivan, M., Fishel, M.L., Tudoran, O.M., Pollok, K.E., Wu, X., and Smith, P.J. (2022). Hypoxia signaling: Challenges and opportunities for cancer therapy. *Seminars in Cancer Biology*, *85*, 185–195.

Jin, C., Zhang, Q., and Lu, W. (2017). Synthesis and biological evaluation of hypoxia-activated prodrugs of SN-38. *European Journal of Medicinal Chemistry*, *132*, 135–141.

Khaiwa, N., Maarouf, N.R., Darwish, M.H., Alhamad, D.W.M., Sebastian, A., Hamad, M., Omar, H.A., Orive, G., and Al-Tel, T.H. (2021). Camptothecin's journey from discovery to WHO Essential Medicine: Fifty years of promise. *European Journal of Medicinal Chemistry*, *223*, 113639.

Kontomanolis, E.N., Koutras, A., Syllaios, A., Schizas, D., Kalagasidou, S., Pagkalos, A., Alatzidou, D., Kantari, P., Ntounis, T., and Fasoulakis, Z. (2021). Basic principles of molecular biology of cancer cell-Molecular cancer indicators. *JBUON*, *26*(5), 1723–1734.

Liang, D., Wu, X., Hasinoff, B.B., Herbert, D.E., and Tranmer, G.K. (2018). Evaluation of Nitrobenzyl Derivatives of Camptothecin as Anti-Cancer Agents and Potential Hypoxia Targeting Prodrugs. *Molecules : A Journal of Synthetic Chemistry and Natural Product Chemistry*, *23*(8).

Liang, S., Li, X., Gao, C., and Zhang, L. (2020). microRNA-based autophagy inhibition as targeted therapy in pancreatic cancer. *Biomedicine & Pharmacotherapy*, *132*, 110799.

Lin, Q., Shi, Y., Liu, Z., Mehrpour, M., Hamaï, A., and Gong, C. (2022). Non-coding RNAs as new autophagy regulators in cancer progression. *Biochimica et Biophysica Acta (BBA) - Molecular Basis of Disease*, *1868*(1), 166293.

Lopacinska-Jørgensen, J., Oliveira, D.V.N.P., Novotny, G.W., Høgdall, C.K., and Høgdall, E. v. (2021). Integrated microRNA and mRNA signatures associated with overall survival in epithelial ovarian cancer. *PLOS ONE*, *16*(7), e0255142.

Miller, D.R., Cramer, S.D., and Thorburn, A. (2020). The Interplay of Autophagy and Non-Apoptotic Cell Death Pathways. *International Review of Cell and Molecular Biology*, *352*, 159.

Ovejero-Sánchez, M., González-Sarmiento, R., and Herrero, A. B. (2021). Synergistic effect of Chloroquine and Panobinostat in ovarian cancer through induction of DNA damage and inhibition of DNA repair. *Neoplasia*, *23*(5), 515–528.

Patil, A.A., Bhor, S.A., and Rhee, W.J. (2020). Cell death in culture: Molecular mechanisms, detections, and inhibition strategies. *Journal of Industrial and Engineering Chemistry*, *91*, 37–53.

Pereira, M., Matuszewska, K., Jamieson, C., and Petrik, J. (2021). Characterizing Endocrine Status, Tumor Hypoxia and Immunogenicity for Therapy Success in Epithelial Ovarian Cancer. *Frontiers in Endocrinology*, *12*, 1520.

Pundir, M., Sharma, A., and Kumar, J. (2022). Phytochemicals used as inhibitors in the treatment of ovarian cancer: A Mini-review. *Materials Today: Proceedings*, *48*, 1620–1625.

Qin, W., Ren, Q., Liu, T., Huang, Y., and Wang, J. (2013). MicroRNA-155 is a novel suppressor of ovarian cancer-initiating cells that targets CLDN1. *FEBS Letters*, *587*(9), 1434–1439.

Rakesh, R., PriyaDharshini, L.C., Sakthivel, K.M., and Rasmi, R.R. (2022). Role and regulation of autophagy in cancer. *Biochimica et Biophysica Acta (BBA) - Molecular Basis of Disease*, *1868*(7), 166400.

Rani, V., and Sengar, R.S. (2022). Biogenesis and mechanisms of microRNA-mediated gene regulation. *Biotechnology and Bioengineering*, 119, 685– 692.

Ruggeri, B. (2021). Cancer (2021): New therapeutic approaches for the treatment of cancer — building on advances in cancer biology and the molecular genetics of cancer. *Current Opinion in Pharmacology*, *60*, 341–345.

Sabzpoushan, S.H. (2020). A System Biology-Based Approach for Designing Combination Therapy in Cancer Precision Medicine. *BioMed Research International*, 21 pages.

Santagostino, S.F., Assenmacher, C.-A., Tarrant, J.C., Adedeji, A.O., and Radaelli, E. (2021). Mechanisms of Regulated Cell Death: Current Perspectives. *Veterinary Pathology*, *58*(4), 596–623.

Shen, Y., Tang, H., Zhan, Y., van Kirk, E.A., and Murdoch, W.J. (2009). Degradable Poly (β-amino ester) nanoparticles for cancer cytoplasmic drug delivery. *Nanomedicine: Nanotechnology, Biology, and Medicine*, *5*(2), 192–201.

Shukla, P., and Singh, K.K. (2021). The mitochondrial landscape of ovarian cancer: emerging insights. *Carcinogenesis*, *42*(5), 663–671.

Sul, O. J., Sung, Y. bin, Rajasekaran, M., Ke, K., Yu, R., Back, S. H., and Choi, H. S. (2018). MicroRNA-155 induces autophagy in osteoclasts by targeting transforming growth factor β-activated kinase 1-binding protein 2 upon lipopolysaccharide stimulation. *Bone*, *116*, 279–289.

Swamy, M.K., Nath, S., Paul, S., Jha, N.K., Purushotham, B., Rohit, K. C., and Dey, A. (2021). Biotechnology of camptothecin production in Nothapodytes nimmoniana, Ophiorrhiza sp. and Camptotheca acuminata. *Applied Microbiology and Biotechnology*, *105*(24), 9089–9102.

Szczepanek, J., Skorupa, M., and Tretyn, A. (2022). MicroRNA as a Potential Therapeutic Molecule in Cancer. *Cells 2022, Vol. 11, Page 1008*, *11*(6), 1008.

Tilija Pun, N., Jang, W. J., and Jeong, C. H. (2020). Role of autophagy in regulation of cancer cell death/apoptosis during anti-cancer therapy: focus on autophagy flux blockade. *Archives of Pharmacal Research*, *43*(5), 475–488.

Wang, F., Shan, S., Huo, Y., Xie, Z., Fang, Y., Qi, Z., Chen, F., Li, Y., and Sun, B. (2018). MiR-155-5p inhibits PDK1 and promotes autophagy via the mTOR pathway in cervical cancer. *The International Journal of Biochemistry & Cell Biology*, *99*, 91–99.

Wang, X., Du, Z.W., Xu, T.M., Wang, X.J., Li, W., Gao, J.L., Li, J., and Zhu, H. (2021). HIF-1α Is a Rational Target for Future Ovarian Cancer Therapies. *Frontiers in Oncology*, *11*, 5495.

Wan, G., Xie, W., Liu, Z., Xu, W., Lao, Y., Huang, N., Cui, K., Liao, M., He, J., Jiang, Y., Yang, B. B., Xu, H., Xu, N., and Zhang, Y. (2014). Hypoxia-induced MIR155 is a potent autophagy inducer by targeting multiple players in the MTOR pathway. *Autophagy*, *10*(1), 70–79.

Wu, C., Zhou, L., Yuan, H., and Wu, S. (2020). Interconnections among major forms of regulated cell death. *Apoptosis*, *25*(9–10), 616–624.

Xia H, Zhao Y. (2020). miR-155 is high-expressed in polycystic ovarian syndrome and promotes cell proliferation and migration through targeting PDCD4 in KGN cells. *Artif Cells Nanomed Biotechnol*. Dec; 48(1):197-205.

Ysrafil, Y., Astuti, I., Anwar, S. L., Martien, R., Sumadi, F. A. N., Wardhana, T., and Haryana, S. M. (2020). MicroRNA-155-5p Diminishes in Vitro Ovarian Cancer Cell Viability by Targeting HIF1α Expression. *Advanced Pharmaceutical Bulletin*, *10*(4), 630.

Zhang, X., Chu, J., Sun, H., Zhao, D., Ma, B., Xue, D., Zhang, W., and Li, Z. (2020). MiR-155 aggravates impaired autophagy of pancreatic acinar cells through targeting Rictor. *Acta Biochimica et Biophysica Sinica*, *52*(2), 192–199.

Zhang Z, Pan X, Yang S, Ma A, Wang K, Wang Y, Li T, Liu S. (2017). miR-155 Promotes ox-LDL-Induced Autophagy in Human Umbilical Vein Endothelial Cells. *Mediators Inflamm.* 9174801.

Zhou, W., Wang, H., Yang, Y., Chen, Z. S., Zou, C., and Zhang, J. (2020). Chloroquine against malaria, cancers and viral diseases. *Drug Discovery Today*, *25*(11), 2012–2022.

Zou, H., Wang, L., Zhao, J., Yuan, Y., Wang, T., Bian, J., and Liu, Z. (2021). MiR-155 promotes cadmium-induced autophagy in rat hepatocytes by suppressing Rheb expression. *Ecotoxicology and Environmental Safety*, *227*.

CIRRICULUM VITAE

Name Surname : Stephen Damola ARIYELOYE

Foreign language : English

Email :

ORCID :

Education and Professional Background:

- 2019-2023 (in view), Anadolu University, Graduate School of Health Sciences, Department of Biochemistry.
- 2022-2023, Erasmus+ Trainee/Student, University Hospital Carl Gustav Carus Dresden (Universitätsklinikum Carl Gustav Carus Dresden) Germany.
- 2021, Erasmus+ Trainee/Student, Center of New Technologies, University of Warsaw, Warsaw, Poland .
- 2018-2019, Graduate/Research Assistant Federal University of Technology, Minna (FUTMINNA) Nigeria.
- 2012-2017, Federal University of Technology, Akure (FUTA), Ondo State, Nigeria, School of Sciences, Department of Biochemistry.

Publications and/or Scientific/Artistic Activities:

- Adeoye, R.A., Garba, S.A., Galadima, M., Ossamulu, I.F and Ariyeloye, S.D. (2019). Prevalence of HIV among women attending selected hospitals in Minna, Niger state, Nigeria. *GSC Biological and Pharmaceutical Sciences*, 9(1), 70-76. Article DOI: 10.30574/gscbps.2019.9.1.0160 **Corresponding Author*
- Ndarubu Tsado A., Jigam, A.A., Akanya, O.H., Ossamulu, O.I, Ariyeloye S.D. (2020). Acute Toxicity Studies and Anti-plasmodial Potentials of Newbouldia laevis and Crateva adansonii in Plasmodium Berghei-infected Mice. *Iranian Journal of Toxicology*, 14(2):93-104. http://dx.doi.org/10.32598/ijt.14.2.636**Corresponding Author*